Aalto University
School of Chemical
Engineering

Viivi Kivelä

FILTRATION OF BIOMASS-BASED GASIFICATION GAS AT ELEVATED TEMPERATURES

Master´s Programme in Chemical, Biochemical and Materials Engineering
Major in Chemical Engineering

Master's thesis for the degree of Master of Science in Technology
submitted for inspection, Espoo, 14 May 2018.

Supervisor Professor Ville Alopaeus

Instructor M.Sc. (Tech) Johanna Kihlman

Aalto University
School of Chemical
Engineering

Aalto University, P.O. BOX 11000, 00076 AALTO
www.aalto.fi

Abstract of master's thesis

Author	Viivi Kivelä
Title of thesis	Filtration of biomass-based gasification gas at elevated temperatures
Degree Programme	Master's Programme in Chemical, Biochemical and Materials Engineering
Major	Chemical Engineering
Thesis supervisor	Professor Ville Alopaeus
Thesis advisor(s) / Thesis examiner(s)	M.Sc. (Tech) Johanna Kihlman
Date 14.05.2018	**Number of pages** 89 +7 **Language** English

Abstract

Literature part of the thesis concerns the combination of biomass gasification process and Fischer-Tropsch synthesis, which can be used to produce liquid biofuels. Cleaning of the gasification gas by filtration and tar reforming is the focus of the work. It is essential to develop an effective and profitable process concept for hot gas cleaning to achieve competitive biofuel production route. The main challenge is to develop stable filtration process that is resistant towards tar components and carbon formation at high temperatures. Heavy tar compounds are decomposed either in the filtration unit or in the following reformer unit. At high temperatures, formed filter cakes are sticky and cleaning of filter medium is challenging. Additionally, the contaminants in the gasification gas complicate the usage of some catalysts. Different catalysts have been studied for gasification gas cleaning applications and catalyst modifications have been tested including different support and promoter additives.

The aim of the experimental part of the thesis was to study the suitability of novel metal filters for hot gasification gas cleaning purpose. Furthermore, the Atomic Layer Deposition (ALD) coating technique was tested in the experiments with nickel catalyst and alumina support. Different process conditions and gas face velocities were studied. It was also tested how sulfur in the gas affects the process. The best result was 55 % conversion for naphthalene and it was achieved with the combination of nickel catalyst and alumina support at 5 bar and at 900 ˚C. The applied gas face velocity was 15 cm/s. However, at these conditions, there occurred carbon formation on the surfaces and finally the reactor was blocked. Without a nickel catalyst, the best conversion achieved for naphthalene was 29 % at same process conditions with the gas face velocity of 12 cm/s. Without a catalyst, less carbon was accumulated on the filter surface and there were no problems related to the reactor clogging.

Keywords Hot gas filtration, gasification gas, tar reforming, metal filter, nickel catalyst, ALD

Aalto University
School of Chemical
Engineering

Aalto University, P.O. BOX 11000, 00076 AALTO
www.aalto.fi

Diplomityön tiivistelmä

Tekijä Viivi Kivelä

Työn nimi Biomassapohjaisen kaasutuskaasun suodatus korkeissa lämpötiloissa

Koulutusohjelma Master's Programme in Chemical, Biochemical and Materials Engineering

Pääaine Chemical Engineering

Työn valvoja Professori Ville Alopaeus

Työn ohjaaja(t)/Työn tarkastaja(t) DI Johanna Kihlman

Päivämäärä 14.05.2018 **Sivumäärä** 89 + 7 **Kieli** Englanti

Tiivistelmä

Diplomityön kirjallisuusosio käsittelee nestemäisten polttoaineiden valmistusta biomassan kaasutuksen ja Fischer-Tropsch-synteesin avulla. Työ keskittyy tutkimaan kaasutuskaasun puhdistuslinjan suodatus- ja reformointiprosesseja. Merkittävä haaste biomassan valmistusprosessin tehokkuuden parantamisessa on saavuttaa stabiili suodatusprosessi. Suodatusprosessin tulisi kestää vaativat prosessiolosuhteet sekä kaasun sisältämien epäpuhtauksien vaikutukset. Raskaat tervayhdisteet hajotetaan joko suodatusvaiheessa tai sitä seuraavassa reformointiyksikössä. Korkeissa lämpötiloissa muodostuvat suodatuskakut ovat tyypillisesti tahmeita ja suodatin on hankala puhdistaa. Korkeissa lämpötiloissa hiiltä kertyy prosessilaitteen pinnoille, mikä voi lopulta johtaa reaktorin tukkeutumiseen. Monia erilaisia katalyyttejä on tutkittu kuuman kaasutuskaasun puhdistamista varten ja katalyyttejä on muokattu esimerkiksi erilaisten tuki- ja lisämateriaalien avulla.

Kokeellisen osion tarkoituksena oli testata uusien metallifilttereiden soveltuvuutta kaasutuskaasun kuumasuodatusta varten. Lisäksi koeajoissa testattiin atomikerroskasvatuksella valmistettuja nikkeliä sekä alumiinioksidia sisältäviä katalyyttipinnoituksia. Myös erilaisia prosessiolosuhteita sekä kaasun pintanopeuksia tutkittiin. Koeajojen avulla saatiin myös lisätietoa rikkiyhdisteiden vaikutuksesta nikkelikatalyytin toimintaan. Paras naftaleenin hajoamiselle saavutettu konversio oli 55 % ja se saavutettiin paksuimmalla nikkelipinnoituksella alumiinioksidin päällä 5 bar paineessa sekä 900 °C lämpötilassa. Kaasun pintanopeus oli 15 cm/s. Näissä olosuhteissa reaktorin hiiltyminen aiheutti kuitenkin ongelmia ja neljän tunnin ajon jälkeen reaktori tukkeutui. Ilman katalyyttiä korkein saavutettu naftaleenin konversio oli 29 % samoissa olosuhteissa, mutta 12 cm/s pintanopeudella. Ilman katalyyttiä, hiiltä kertyi reaktoriin huomattavasti vähemmän eikä reaktorin tukkeutumista tapahtunut.

Avainsanat Kaasun suodatus korkeissa lämpötiloissa, kaasutuskaasu, tervojen hajottaminen, metallisuodatin, nikkeli-katalyytti, ALD

Foreword

This master's thesis was carried out between October 2017 and April 2018 in the team of Catalyst Technologies at VTT Technical Research Centre of Finland. The thesis was part of the EU-funded project named COMSYN.

I would like to thank Pekka Simell and Johanna Kihlman for offering me the opportunity to do my master's thesis for VTT. I would also like to thank my advisors Johanna Kihlman and Sanna Tuomi for suggesting this topic for the thesis, for giving me valuable information related to the topic and for helping me with the challenges met during the work. I appreciate the comments and feedback that I got from my supervisor Professor Ville Alopaeus. I would like to thank Mari-Leena Koskinen-Soivi, Päivi Jokimies, Katja Heiskanen and Petri Hietula for guiding me with the equipment and practical issues during the experimental work. I am also grateful to Matti Putkonen for making the catalyst coatings and for introducing the ALD coating technology. My compliments to the whole team of Catalyst Technologies for supportive and helpful atmosphere. Additionally, I want to thank my family and friends for supporting me during all the stages of the work.

Espoo, 14 May 2018

Viivi Kivelä

Table of Contents

List of abbreviations

ALD	Atomic Layer Deposition
$E_{cleaning}$	Cleaning efficiency of the filter [-]
COMSYN	Compact Gasification and Synthesis process for Transport Fuels
X_i	Conversion of the component i [%]
CTI	Critical thickness index [-]
A	Cross-sectional are of the filter [m^2]
FT	Fischer-Tropsch
GHSV	Gas hourly space velocity [s^{-1}]
m_i	Mass of the component i [g]
λ	Mean free path [m]
$P_{measured}$	Measured pressure inside the reactor [Pa]
$F_{i,\,in}$, $F_{i,\,out}$	Molar flow before and after reactor [mol/s]
M_i	Molar mass of the component i [g/mol]
V_m	Molar volume of the component [m^3/mol]
n_i	Number of moles [mol]
ε_c	Porosity of the dust cake [-]
Δp_m	Pressure drop across the filter medium [Pa]
Δp_c	Pressure drop across the temporary dust cake [Pa]
p_2	Pressure of gas after the filter [Pa]
p_1	Pressure of gas before the filter [Pa]

U	Gas face velocity [m/s]
α	Resistance of the cake [m^{-2}]
β	Resistance of the filter medium [m^{-1}]
k_C	Permeability of the filter cake [m^2]
k	Permeability of the porous medium [m^2]
$P_{set\ point}$	Setup pressure for the reactor [Pa]
z	Thickness of the porous medium [m]
z_c	Thickness of the cake [m]
ΔP	Total pressure drop across the filter [Pa]
μ	Viscosity of the fluid [Pa·s]
Q	Volumetric flow rate of the fluid [m^3/s]
Q_{dry}, Q_{wet}	Volumetric flowrate of the dry gas and wet gas [m^3/s]
$vol\text{-}\%_i$	Volumetric composition of the component I [%]
V_i	Volume of the component i [m^3]
WGSR	Water-gas shift reaction
Y_i	Yield of the component i [%]

1 Introduction

Increasing energy consumption and diminishing of finite fossil fuel reserves have caused high demand for alternative energy sources. It is essential to find more environmental friendly and sustainable energy options for future (Enerdata, Global Energy Statistical Yearbook, 2017; Rodionova, et al., 2016). Usage of fossil sources is harmful for environment and it affects the climate (Höök & Xu, 2013). There are several potential carbon dioxide neutral energy options requiring further studies and development. Thermal processes are able to convert biomass into more valuable forms for further processes (Sikarwar, et al., 2017; Sansaniwal, et al., 2017). Thermal conversion can proceed through some of the three main pathways, which include combustion with oxygen, pyrolysis without oxygen and gasification that utilizes controlled amount of oxygen (McKendry, 2002a). When gasification of biomass is combined with the Fischer-Tropsch synthesis, it can be used to produce liquid transportation fuels (Sikarwar, et al., 2017; Sansaniwal, et al., 2017).

Biomass gasification produces gasification gas, which needs accurate cleaning before it is suitable for the following synthesis process. The main components that need to be removed from the gas include particulates, ash, tars, sulfur compounds and nitrogen compounds (Woolcock & Brown, 2013; Asadullah, 2014). Tar compounds might either damage the downstream process equipment or impair the catalyst behavior. Cleaning line for gasification gas needs to be studied more to find the most suitable equipment and optimum process conditions. Cleaning starts with a filter unit usually at temperatures between 300-600 ˚C. Next step is to remove tars, lighter hydrocarbons and ammonia by a reformer unit. Reforming is typically carried out at same temperatures as gasification and thus the gas is heated again after the filtration. Process efficiency can be enhanced by increasing the filtration temperature up to 800 ˚C. Optimization of the process conditions is important to achieve energy efficient process and to minimize additional heating and cooling (Tijmensen, et al., 2002; Simell, et al., 2014).

This thesis studies the behavior of high temperature filtration and catalytic tar decomposition as a part of the EU-funded project named COMSYN (Compact Gasification and Synthesis Process for Transport Fuels). The purpose of the COMSYN project is to develop a competitive biomass gasification process combined with Fischer-Tropsch synthesis to produce transportation fuels from biomass feedstock (http://www.vtt.fi/sites/BTL2030, September 2017). The thesis aims to study activity of the filters towards tar decomposition. In the literature part, different steps of the gasification and synthesis process are discussed. The report concentrates to study the gas cleaning line and in more detail the newest developments in the field of hot gas filtration.

In the experimental part of the thesis, high temperature filtration was tested with the novel metallic filters. Some Atomic Layer Deposition (ALD) catalyst coatings, made of nickel, were also tested and analyzed during the laboratory experiments. The activity and stability of the filters were studied related to catalyst deactivation, tar decomposition and reactor clogging. Gasification gas and model tar mixture with the specific compositions were used in the tests. The experimental system limited the tests so that the effects of the actual ash and filter cleaning on the filter performance were not studied in these experiments. Additionally, the applied gas face velocities were higher than in typical experiments.

2 Process description

Gasification of biomass produces renewable liquid fuels when integrated with the Fischer-Tropsch (FT) synthesis. FT-synthesis converts the gasification gas into suitable hydrocarbons, which can be upgraded into fuels. Gasification gas consists mainly of syngas including hydrogen (H_2), carbon monoxide (CO), carbon dioxide (CO_2), water (H_2O) and methane (CH_4) (Pallozzi, et al., 2016; Hamelinck, et al., 2004). Furthermore, there are impurities, such as particulates, tars, hydrogen sulfide (H_2S), light hydrocarbons and ammonia (NH_3), which need to be removed before the FT-synthesis can take place (Hamelinck, et al., 2004).

Concept of the biofuel production process and the main process steps are illustrated in the Figure 1. From the Figure 1, it can be seen that the fuel production process requires multiple process units in addition to gasification and synthesis steps to convert raw materials into liquid fuels. The main units include raw material pretreatment process, gasifier, gas cleaning process, synthesis and upgrading units (Hamelinck, et al., 2004). These units are introduced briefly in the following sections. The aim is to go through the chemistry, the used catalysts and the process configurations of each process step. Cleaning units and especially the filtering unit are discussed in more detail later in the report but the main points are introduced already in this section.

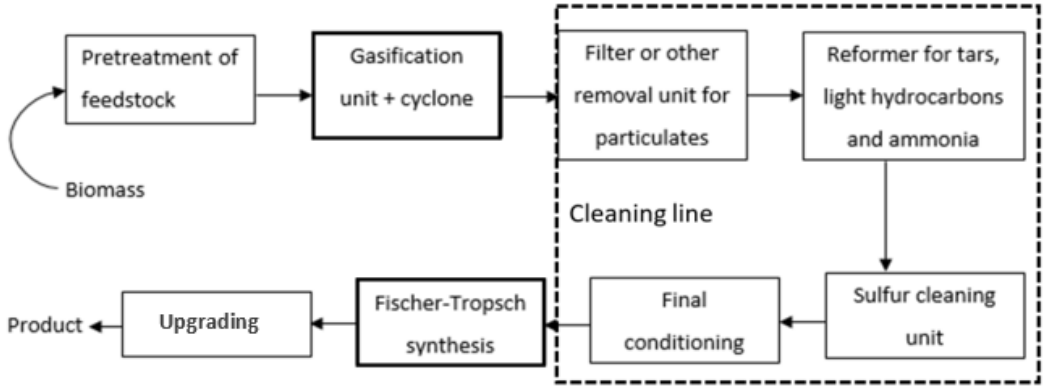

Figure 1. The main process units in the liquid fuel production by biomass gasification and Fischer-Tropsch synthesis.

2.1 Gasification unit

Drying and size reduction are usually needed for the pretreatment of gasification raw materials (Ojeda & Rojas, 2010). In gasification of biomass, endothermic reactions, typically occurring at temperatures between 700-1000 ˚C, convert solid carbonaceous raw materials into gas (McKendry, 2002b). There is less oxygen present than in the combustion and partial oxidation occurs with air to fuel ratios around 1.5:1. This ratio depends on the feedstock and gasification process properties (McKendry, 2002a; Rajvanshi, 1986). Gasification agent is typically either oxygen, steam or a mixture of these two and it participates in the biomass oxidation reactions (Sikarwar, et al., 2017). Heat is added either directly or indirectly to the system and pressurized system should be applied if the following cleaning units and synthesis reactor are performed at high pressure (Kaisalo, 2017; Ojeda & Rojas, 2010).

2.1.1 Chemistry

Gasification process consists of wide set of different drying, pyrolysis or devolatilization, combustion and gasification reactions that occur in parallel and are dependent on the process conditions (de Souza-Santos, 2004; Sikarwar, et al., 2017; Ojeda & Rojas, 2010). The most essential reactions during the gasification are

introduced below. Gasification (1) produces the following main products at process temperatures between 700-1000 ˚C. If air is used as a gasification agent, there is higher amount of nitrogen present in the gas (Gil, et al., 1999; Tuomi, et al., 2015).

Biomass, gasifying agent → CO, H_2, CO_2, CH_4, H_2O, N_2, C, minor contaminants (1)

The main reactions that take place during biomass gasification are the water-gas shift reaction (2), oxidation (3), partial oxidation (4), steam gasification (5) and (6), Boudouard (7) and methanation (8) and (9) reactions (McKendry, 2002b; André, et al., 2005).

$$CO(g) + H_2O(g) \rightleftharpoons CO_2(g) + H_2(g) \quad (2)$$

$$C(s) + O_2(g) \rightleftharpoons CO_2(g) \quad (3)$$

$$C(s) + \frac{1}{2}O_2(g) \rightleftharpoons CO(g) \quad (4)$$

$$C(s) + H_2O(g) \rightleftharpoons CO(g) + H_2(g) \quad (5)$$

$$C(s) + 2H_2O(g) \rightleftharpoons CO_2(g) + 2H_2(g) \quad (6)$$

$$C(s) + CO_2(g) \rightleftharpoons 2CO(g) \quad (7)$$

$$CO(g) + 3H_2(g) \rightleftharpoons CH_4(g) + H_2O(g) \quad (8)$$

$$CO_2(g) + 4H_2(g) \rightleftharpoons CH_4(g) + 2H_2O(g) \quad (9)$$

At temperatures around 100 ˚C, feedstock starts to lose its moisture to form steam (de Souza-Santos, 2004). This steam can take part in the water-gas shift reaction (2) to produce carbon dioxide and hydrogen. Devolatilization and pyrolysis take place approximately at temperatures between 120-700 ˚C and they decompose the biomass mainly into volatile light gases, tars and char (de Souza-Santos, 2004; Rajvanshi, 1986). During the combustion (3) and (4), the organic compounds containing carbon produce carbon dioxide and carbon monoxide with the help of oxygen. At the temperatures between 500-1300 ˚C, char and steam react together to form carbon dioxide, hydrogen and some carbon monoxide as shown in the equations (5) and (6). Carbon and carbon dioxide can react to form carbon monoxide (7). Methanation reactions (8)

and (9) are catalytic reactions of carbon monoxide, carbon dioxide and hydrogen to form gases with high methane content (Zennaro, et al., 2013). Water-gas shift reaction (WGSR) (2) determines the H_2/CO ratio for the gas (Maitlis, 2013). The FT-synthesis requires a ratio of 2:1 (Zennaro, et al., 2013).

Gasification reactions do not necessarily need a catalyst, but some catalyst is often applied to improve the process conversion, selectivity and reaction rates. Additionally, lower temperatures might be sufficient for the process when a catalyst is applied. Usually, solid metal catalysts supported by inorganic carriers are suitable for these applications (Zennaro, et al., 2013; Ojeda & Rojas, 2010). Ojeda et al. (2010) recommended Rh, Ni and Pt as the most active metal catalysts for biofuel gasification systems (Ojeda & Rojas, 2010). In addition, catalysts with high contents of nickel are suitable for gasification applications (Zennaro, et al., 2013; Ojeda & Rojas, 2010).

2.1.2 Process configuration

Efficient biomass gasification process usually demands high pressure and temperature (Higman & van der Burgt, 2003). Process is typically carried out in a fixed bed or fluidized bed gasifier reactor with an integrated downstream cyclone for the primary removal of solid components. The two main types of fixed bed gasifier reactors are shown in the Figure 2. Fixed bed gasifier can be either co-current or counter current system depending on how the feedstock and gasifying agent are fed to the unit in relation to each other (Asadullah, 2014).

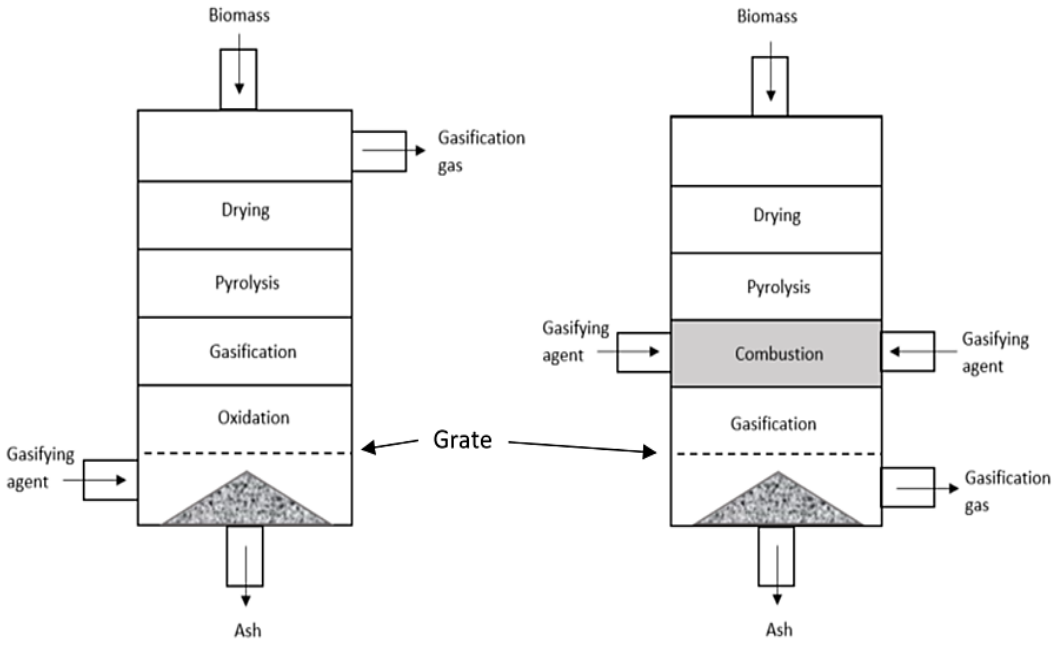

Figure 2. (a) Updraft fixed bed and (b) downdraft fixed-bed gasifiers.

In fixed bed gasifiers, the feedstock moves slowly downward in a bed due to gravity and finally stays on a grate. There is a gasification agent flowing through the grate to heat the material and to transport the product gas out of the reactor (Basu, 2013; Higman & van der Burgt, 2003). Problems of counter-current gasifier are related to the product gas that has high content of tar compounds. This is because the feedstock inlet is quite close to the product gas outlet (Higman & van der Burgt, 2003). In co-current system, these issues are not so crucial because gasifying agent and feedstock meet in the inlet area. Anyway, there might be issues related to process scale-up due to the challenges of controlling the gasification agent, biomass and temperature distribution in the system (Asadullah, 2014).

Fluidized bed gasifiers are the most used systems for biomass gasification due to their potential for efficient mass and heat transfer. They can be divided into circulating, bubbling and dual fluidized bed gasifiers. Basic method of fluidized bed gasifier is shown in the Figure 3 (Higman & van der Burgt, 2003). The gasification agent transports the biomass through the reaction section, which consist of a bed of granular solids (Basu, 2013). The gas flows upward in the reactor and leaves from the top with

the gasifying agent. Most of the bed material and solid feedstock in the product gas is separated in a cyclone and recycled to the bottom of the gasifier (Hannula & Kurkela , 2013). Bubbling fluidized bed has higher flow rates, which causes the bubbling of the bed. In dual bed gasifier, the combustion of char and gasification take place in separate sections. Usually, gasification in fluidized bed gasifier is carried out at temperatures in the range of 750-950 ˚C (Higman & van der Burgt, 2003; Basu, 2013).

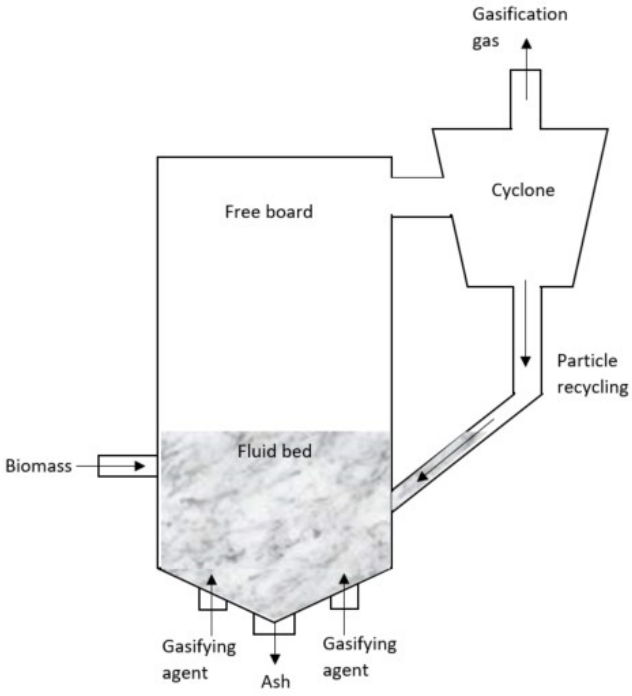

Figure 3. The method of fluidized bed gasifier.

Used temperature and bed material have both significant effect on the product gas properties (Weerachanchai, et al., 2009). One important function of bed material is to control the temperature profile in the gasifier (Siedlecki, et al., 2009). In addition to this, some bed materials are able to improve tar decomposition. For example, dolomite and magnesite are suitable bed materials for biomass gasification due to their catalytic nature and stability. By utilizing catalytically active bed materials, tar amounts in the product gas can be reduced already before the filtration unit (Siedlecki, et al., 2009; Zhou, et al., 2017). Mineral bed materials enable to reduce agglomeration and help to avoid blockage of reactor that might cause problems with many general bed materials such like quartz sand (Siedlecki, et al., 2009; Zhou, et al., 2016).

2.2 Gas cleaning line

Fischer-Tropsch synthesis requires the gas with high purity level and thus the contaminants mentioned earlier need to be removed carefully (Tijmensen, et al., 2002). The four main steps of the cleaning process include particulates removal, reforming, sulfur removal and final conditioning. As the cleaning units have varying optimum temperatures and pressures, the optimization of the entire gas cleaning line is important for the process feasibility. Hot gas cleaning processes at temperatures between 700-900 ˚C are favoured due to energy efficiency of the process line (Simell, et al., 2014; Abdoulmoumine, et al., 2015).

2.2.1 Filtration

Removal of particulates begins usually with a simple cyclone, which takes advantage of rotational effects and gravity to separate the solids, such as residual bed material, from the gas. Cyclones work usually well for preliminary separation (Stevens, 2001; Seville, 1997). The unit after a cyclone, typically the filtration unit, removes most of the ash and particulates (Asadullah, 2014). Usually, some kind of ceramic or metal candle filters are applied (Simeone, et al., 2013; Chung, et al., 2003). Other options for hot gas cleaning include electrostatic precipitation and granular bed filters (Sikarwar, et al., 2017; Seville, 1997).

Electrostatic filters separate the particles by using electrical forces. High voltage electrical charges are set to circulate between two electrodes. The gas particles are charged and moved to the earthed electrode to be neutralized. Neutralized particles are recovered by an electrode and a rapping unit (Villot, et al., 2012). Precipitators are flexible with particulate size but they need more studies to be suitable to use at high temperature and pressure (Seville, 1997). Granular bed filters utilize grain of specific size applied either in the form of fixed, fluidized or moving beds. These filters are not so efficient for smaller particles and there are often problems related to cleaning and complexity of the systems (Villot, et al., 2012; Xiao, et al., 2013). For lower temperatures, wet scrubbing process is suitable, but it produces large amounts of

contaminated waste stream and thus it is not an environmentally friendly option (Sansaniwal, et al., 2017).

In the COMSYN project, the hot gas filtration is used for removing particulates from the gas (http://www.vtt.fi/sites/BTL2030, September 2017). Filter is a relatively simple and flexible process option when compared to the other hot gas cleaning processes (Sansaniwal, et al., 2017). Filter unit can include different filter materials, catalysts and structures. Fabric filter materials are suitable only for low temperatures (Seville, 1997). Both metal and ceramic filters are studied for particulates removal in gasification conditions (Stevens, 2001). The structure of a simplified candle filter arrangement can be seen in the Figure 4, modified from Seville, et al., 2003. In the Figure 4, it is shown that the hot gas flows from outside of the hollow cylindrical filter element to inside forming a filter cake on the outer surface. Reverse pulses are utilized to clean the filter medium (Seville, 1997).

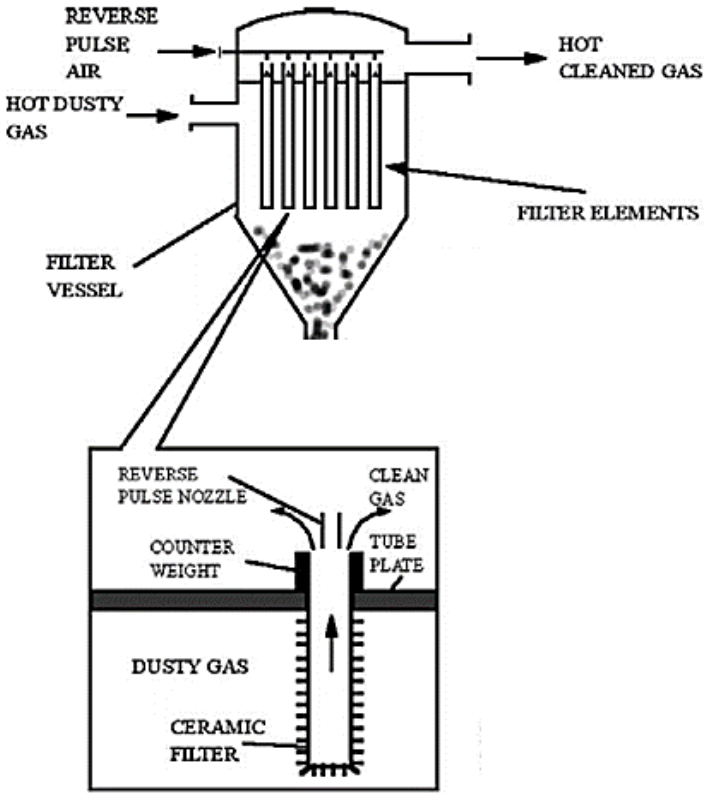

Figure 4. The structure of a simplified candle filter arrangement (Modified from Seville, et al. 2003).

2.2.2 Reformer unit

Reformer unit is responsible for removing tars, NH_3 and hydrocarbons from the gas. As mentioned earlier, tars are contaminants that cannot be present in the FT-synthesis. In the gasification gas, tars comprise a group of hundreds of different aromatic and polyaromatic hydrocarbons (Moersch, et al., 2000). Tars are removed typically either by scrubbing, thermal cracking or catalytic cracking (Hamelinck, et al., 2004).

Scrubbing is a method that works at relatively low temperatures and produces wastewater. The selective scrubbing solution contacts with the gas to separate the desired components (Boerrigter, et al., 2002; Bergiorno, et al., 2003). In the scrubbing process, temperature is decreased so that the heavier tar components can condense to fine aerosols and absorb into water. Lighter tar components absorb into water due to their water solubility (Woolcock & Brown, 2013).

Thermal cracking of tar compounds without a catalyst with reasonable velocities requires temperature above 1000 °C (Milne & Evans, 1998; Sikarwar, et al., 2017). Thermal cracking produces problematic soot and demands materials with good thermal resistivity (Hamelinck, et al., 2004). Thermal cracking proceeds according to the equations (10) and (11) to form smaller hydrocarbons, hydrogen and water (Devi, et al., 2005).

$$pC_nH_x(\text{tar}) \xrightarrow{\text{heat}} qC_mH_y(\text{smaller tar}) + rH_2 \quad (10)$$

$$pC_nH_xO_y(\text{tar}) \xrightarrow{\text{heat}} qC_mH_z(\text{smaller tar}) + rH_2O \quad (11)$$

Catalytic cracking with dolomite or Ni based catalysts are proved to be promising options for tars removal (Hamelinck, et al., 2004). Tar decomposition includes many competitive reactions overlapping with each other. The water-gas shift (2), steam gasification (5) and (6) and Bouduard (7) reactions were introduced already in the gasification part. Additionally, steam reforming (12) and (13), dry reforming (14),

hydrocracking (15) and (16) and carbon formation (17) and (18) reactions take place (Li & Suzuki, 2009; Abdoulmoumine, et al., 2015).

$$C_nH_x(tar) + nH_2O \rightarrow nCO + \left(n + \frac{x}{2}\right) H_2 \quad (12)$$

$$C_nH_xO_y(tar) + (n - y)H_2O \rightarrow nCO + \left(n + \frac{x}{2} - y\right) H_2 \quad (13)$$

$$C_nH_x(tar) + nCO_2 \rightarrow 2nCO + \left(\frac{x}{2}\right) H_2 \quad (14)$$

$$C_nH_x(tar) + \left(\frac{4n - m}{2}\right) H_2 \rightarrow nCH_4 \quad (15)$$

$$C_nH_xO_y(tar) + mH_2 \rightarrow nCH_4 + yH_2O \quad (16)$$

$$C_nH_x(tar) \rightarrow nC + \left(\frac{x}{2}\right) H_2 \quad (17)$$

$$C_nH_xO_y(tar) \rightarrow nC + \frac{1}{2}(x - 2y)H_2 + yH_2O \quad (18)$$

Decomposition of tars can occur through hydrocracking in which hydrogen is used to crack tars into methane and water. Steam reforming reactions (12) and (13) utilize dehydrogenation to produce carbon monoxide and hydrogen. Dry reforming (14) converts tars into carbon monoxide and hydrogen by consuming steam and carbon dioxide. Optimum process conditions need to be found to avoid carbonization of the reactor and to maximize the conversions of reforming reactions (Simell, et al., 2014; Li & Suzuki, 2009; Abdoulmoumine, et al., 2015).

2.2.3 Other cleaning and conditioning of the gas

Alkali metals need to be removed from the syngas because they can cause corrosion, catalyst poisoning or fouling. These components are highly volatile and reactive (Balonek, et al., 2010; Dayton, et al., 1995). Alkali metals are usually removed from the gasification gas by high temperature adsorption or condensation (Woolcock & Brown, 2013). Adsorption is sufficient also at higher temperatures when a sorbent has right properties to tolerate the process conditions, regeneration, adsorption and loading with reasonable reaction rate and stability (Sikarwar, et al., 2017; Punjak, et al., 1989).

For example, montmorillonite with $MgOH_2$ and activated alumina is used in gasification gas adsorption (Dou, et al., 2007). Often these sorbents can also remove chlorine from the gas (Sikarwar, et al., 2017; Dou, et al., 2007).

Nitrogen in the gasification product gas is usually in the forms of ammonia and hydrogen cyanide (Pinto, et al., 2010). Removal of nitrogen compounds requires a catalyst and occurs either through thermal degradation or selective oxidation (Pinto, et al., 2010; Sikarwar, et al., 2017; Juutilainen, et al., 2006). Many of the catalysts used in the reformer are also suitable for removing nitrogen compounds. For example, dolomite, zirconia with alumina and nickel catalysts have shown their suitability for removal of ammonia (Sikarwar, et al., 2017; Juutilainen, et al., 2006).

Sulfur compounds are usually removed from the hot gas by chemical or physical adsorption (Westmoreland & Harrison, 1976). Hydrogenation is first needed to convert COS to H_2S. (Sikarwar, et al., 2017). Rectisol® and Selexol™ are the most widely used physical solvent processes (Zennaro, et al., 2013). Selexol™ process utilizes double absorption and stripping towers for scrubbing hydrogen sulfide and for removing carbon dioxide. Rectisol® is quite similar process but there is one extra unit added for methanol solvent refrigeration. Hydrogen sulfide is removed in the first regeneration column and carbon dioxide in the second column by stripping with decreasing pressure of the methanol (Mohammed, et al., 2014).

2.3 Fischer-Tropsch synthesis

In the FT-synthesis, the mixture of hydrogen and carbon monoxide is converted mainly into linear long chain alkanes and alkenes with the help of a catalyst. The produced liquid hydrocarbons can be used for producing fuels or chemicals after appropriate upgrading processes (Maitlis, 2013). In the following section, chemistry and process equipment of the FT-synthesis are introduced.

2.3.1 Chemistry

The Fischer-Tropsch synthesis is a quite complicated process including many primary and secondary polymerization reactions. During the exothermic reaction, monomer CH_x* surface species are produced from CO and H_2. There are chain initiators participating in the chain growth reactions to form especially paraffins and olefins. The synthesis can be summarized by the three main reactions that include paraffin (19), olefin (20) and alcohol formations (21) (González-Carballo & Fierro, 2010). The ratio of hydrogen and carbon monoxide has a significant effect on the reactions occurring during the synthesis (Pour, et al., 2010).

$$nCO + (2n + 1)\, H_2 \rightarrow C_nH_{2n+2} + nH_2O \quad (19)$$

$$nCO + 2nH_2 \rightarrow C_nH_{2n} + nH_2O \quad (20)$$

$$nCO + 2nH_2 \rightarrow C_nH_{2n+2}O + (n - 1)H_2O \quad (21)$$

2.3.2 Process configurations

The best process option for FT-synthesis depends on the process conditions, used catalyst and desired products. The commonly employed reactors are multi-tubular fixed bed, circulating fluidized bed, fixed fluidized bed and fixed slurry bed reactors (Sie & Krishna, 1999). Synthesis can be applied in fluidized bed reactor at high temperatures between 300-350 °C. With tubular or slurry phase reactors, lower temperatures around 200-240 °C are typically used. With high reactor temperatures, products with shorter molecule chains, such as olefins and gasoline, are produced (Maitlis, 2013). If heavy linear waxes are the desired products, FT-process at lower temperatures is preferred (Sie & Krishna, 1999; Speight, 2011).

FT-synthesis requires catalyst that is able to catalyze CO hydrogenation to produce long chain hydrocarbons. Iron and cobalt are widely used metal catalysts in the Fischer-Tropsch synthesis (Ojeda & Rojas, 2010; Li, et al., 2002). The cobalt catalyst includes fine metal supported particles on an oxide surface. Wide surface area enhances the activity but allow also impurities to adsorb on the surface. If long-chain

hydrocarbons such as waxes are formed, they need to be cracked to produce liquid fuels. The synthesis takes place at the interface of metal and oxide (Maitlis, 2013). Some oxide compounds, for example alumina and silica, are used to support catalysts (Maitlis, 2013). These supports form large porous surfaces in which the catalytically active components are deposited and stabilized as nanoparticles (Romar, 2015). Sometimes promoting effects are utilized in the synthesis by adding some promoter material. Promoters can for example increase the amount of active sites by improving metal dispersion. Different combinations of both catalyst, supporting and promoting materials are studied for better catalyst performance. For example, Fe_2O_3 catalyst with MnO_2 promoter have shown good behavior in the FT-synthesis (Zhang, et al., 2016).

3 Properties of the gasification gas

Gasification gas has variable compositions and includes different contaminants depending on process design, type of biomass and process conditions. This chapter concentrates to discuss about the composition and contaminants of the gas in more detail. The purpose is also to evaluate the gas quality requirements for different syngas applications, especially for the FT-synthesis. For FT-synthesis, the cleaning of the gasification gas is essential and high accuracy cleaning is required when compared to other process pathways (Asadullah, 2014). Gas obtained from biomass gasification process can be utilized in many applications when different conversion technologies are applied as can be seen in the Figure 5 and Figure 6 (Premium Engineering, 2016; Spath & Dayton, 2003).

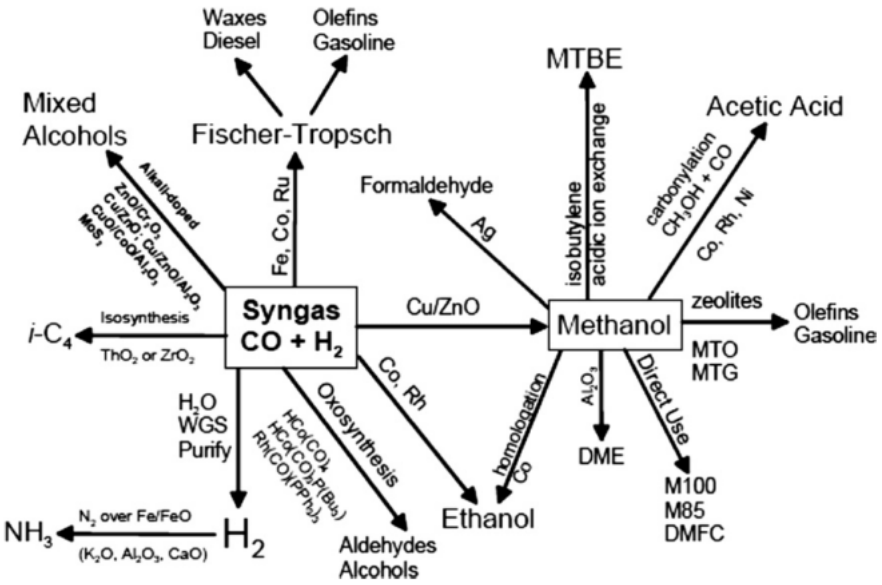

Figure 5. The different conversion technologies applied for the syngas (Spath & Dayton, 2003).

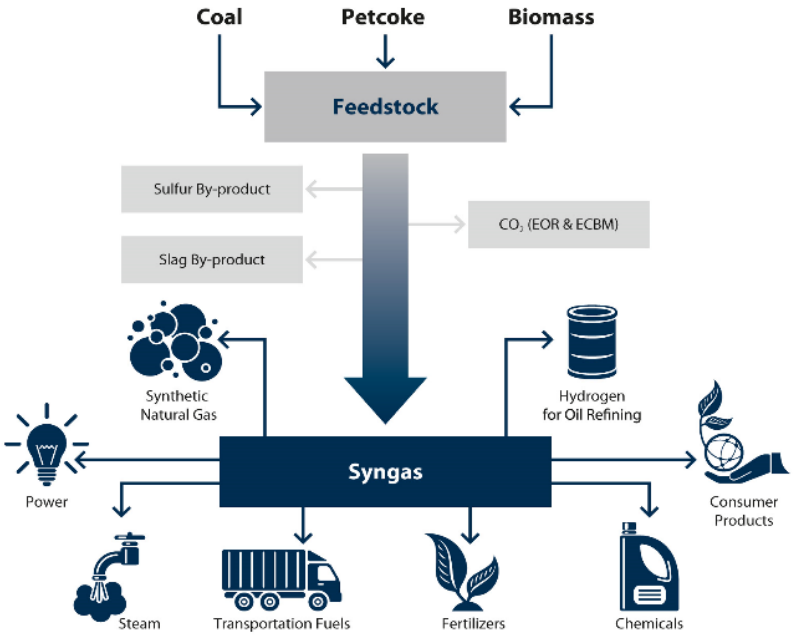

Figure 6. The most important applications for syngas (Premium Engineering, 2016).

As can be seen from the figures above, syngas has many applications of which transportation fuels is only one option. Syngas can be used for example to produce hydrogen, methanol or mixed alcohols (Premium Engineering, 2016; Mondal, et al., 2011). Applications of syngas include power production, fuels, fertilizers, chemicals and many other options (Premium Engineering, 2016).

There are also variable options for gasification feedstock, of which biomass is the most suitable one due to the environmental and sustainability perspectives (Premium Engineering, 2016). In Finland, the most attractive feedstock include woody biomass and waste streams of forest industry (Hannula & Kurkela , 2013). COMSYN project concentrates to develop efficient steam gasification process combined with hot gas filtration, catalytic reforming, sulfur removal and FT-synthesis to produce liquid transportation fuels from biomass residues (http://www.vtt.fi/sites/BTL2030, September 2017).

3.1 Composition of the gas

As mentioned above, the gas properties are affected strongly by the gasification process conditions and other parameters. In the experimental part of this thesis, the syngas with determined uniform composition is used to test the filtration unit. This is for simplifying the tests, but usually in the actual process, the situation is quite different. For demonstrating the variations between the gas compositions, a few examples are shown in the Table 1 (Kurkela, et al., 2016; Tuomi, et al., 2015). Differences depend especially on the gasifying agent, fuel properties, bed material, catalyst and process conditions (Li, et al., 2004; Mathieu & Dubuisson, 2002; Sikarwar, et al., 2017).

Table 1. Two examples of biomass gasification gas compositions (Kurkela, et al., 2016; Tuomi, et al., 2015).

Circulating fluidized bed gasifier for wood residues		Dry gas product composition (vol-%) (Kurkela, et al., 2016)					
Gasification agent and bed material	Conditions (˚C, bar)	H_2	CO	CO_2	CH_4	N_2	C_2H_2 - C_2H_6
Steam/oxygen, sand and dolomite	900, 1	29-32	17-19	33-35	6-8	7-11	0-2
Bubbling fluidized bed gasifier for wood and bark		Dry gas product composition (vol-%) (Tuomi, et al., 2015)					
Steam, Sand or dolomite	Conditions (˚C, bar)	H_2	CO	CO_2	CH_4	N_2	C_2H_2 - C_2H_6
	790-810, 1	44-52	18-24	20-24	5-9	0	1-5

When air is used as a gasification agent, there is more nitrogen in the gasification gas that needs to be removed before synthesis and thus the product yield is decreased. In addition, gasification temperature has a great effect to the gasification gas

composition. By increasing the residence time, there is more time for tars cracking (Farzad, et al., 2016).

3.2 Contaminants in the gas

The main harmful contaminants found in the gasification gas include particulates, alkali compounds, tars, nitrogen compounds, sulfur and low molecular weight hydrocarbons. Some of these components need to be removed due to the emission regulations and some due to the possible damages occurring in the following downstream equipment (Sansaniwal, et al., 2017). These components are discussed briefly in the following sections. The composition of contaminants depends for example on the gasification feedstock. Many different contaminants are present in the biomass feedstock. This helps to understand the wide range of contaminants that appear in the gasification product gas as well. Example of the gas contaminants is shown in the Table 2, based on the experiments conducted by Kurkela et al. (2016). Table 3 shows the estimated maximum allowable values for contaminants in the FT-synthesis.

Table 2. Example of amounts of gasification gas contaminants (Kurkela, et al., 2016).

Circulating fluidized bed gasifier for wood residues		Main impurities in the gas (Kurkela, et al., 2016)				
Gasification agent and bed material	Conditions (˚C, bar)	COS (ppmv)	NH_3 (ppmv)	HCN (ppmv)	Tars and benzene (g/m^3n)	H_2S (ppmv)
Steam/oxygen, sand and dolomite	900, 1	1-4	2730-4970	10-17	17-20	100-172

Table 3. Estimated maximum values for amounts of main impurities in FT-synthesis feedstock. (Tijmensen, et al., 2002; Boerrigter, et al., 2002)

Contaminants	Sulfur (H_2S, COS)	Halides	Nitrogen (NH_3, HCN)	Tars	Particulates	Alkalis
Tolerable amount [ppb]	< 1	< 10	< 20	Below dew point	Not-detectable	< 10

As can be seen in the Table 2 and Table 3, amounts of sulfur, nitrogen and tar compounds need the most significant decrease before the synthesis. In the Table 4, some values for compositions of gasification gas before and after reformer unit and before and after filtration unit are shown. Reformer unit removed high amounts of tars when precious metal catalysts were used but ammonia and sulfur components stayed almost constant. When a catalytic filter medium was used, amount of tars was not decreased as much as in the separate reformer unit.

Table 4. Examples of gasification gas compositions before and after reformer and filter units (Simell, et al., 2014; Nacken , et al., 2015).

Precious metal catalysts on modified zirconia	The gas composition and the main impurities in the gas before and after a reformer unit (vol-%) (Simell, et al., 2014)						
Before the reformer	H_2	CO	CO_2	CH_4	N_2	C_2H_2 - C_2H_6	H_2O
	16-24	13-19	18-21	4-7	7-21	0-0.7	21-32
	COS (ppmv)	NH_3 (vol-%)		HCN (vol-%)		Tars and benzene (vol-%)	H_2S (ppmv)
	2-5	0.08-0.12		0.001-0.004		0.2-0.4	40-120
After the reformer	H_2	CO	CO_2	CH_4	N_2	C_2H_2 - C_2H_6	H_2O
	20-26	11-17	16-19	1-3	8-24	0.002-0.0028	26-37
	COS (ppmv)	NH_3 (vol-%)		HCN (vol-%)		Tars and benzene (vol-%)	H_2S (ppmv)
	2-5	0.05-0.08		0.001-0.003		0.001-0.008	40-120
Catalytic filter candle CombCatFil, NiO on MgO-Al_2O_3 layer ceramic foam filter candle at 800 ˚C	Composition (vol-% per dry gas) (Nacken , et al., 2015)						
Before the filter	H_2	CO	CO_2	CH_4	Tars (g/nm^3)		
	10	12	11	5	7.9		
After the filter	H_2	CO	CO_2	CH_4	Tars (g/nm^3)		
	52	22	21	5	1.5		

3.2.1 Particulates

Particulates are solid components that in the gasification gas mainly consist of ash, char and gasifier bed material. The inorganic compounds derived from the mineral part of the biomass often form ash. These solid materials tend to damage downstream processes through corrosion, abrasion and catalyst inactivation (Asadullah, 2014; Sikarwar, et al., 2017). Char contains the biomass that has not converted completely during the gasification and is thus in the form of micron size dust (Asadullah, 2014).

Inorganic part of the particulates consists of calcium, potassium, silicon, kalium, natrium, magnesium and iron components (Szemmelveisz, et al., 2009; Gustafsson, et al., 2007). There can be some components present in the ash, such as potassium salts, that may vaporize at high temperatures, which complicates their removal (Stevens, 2001). The gas produced by the fluidized bed gasifier generally contains more particulates than the gas from the fixed bed gasifier (Asadullah, 2014).

3.2.2 Tars

Tars are condensable organic compounds present in the gasification gas. They comprise compounds from lighter hydrocarbons to heavier aromatic hydrocarbons. The latter of which are more difficult to remove (Li & Suzuki, 2009). Different tar compounds can be classified for example by their solubility, by their tendency of condensation and by the process temperature as shown in the Figure 7 (Li & Suzuki, 2009). Tars are produced in the gasifier by a complex group of reactions. At higher temperatures, secondary reactions produce light oxygenates, hydrocarbons, aromatics and olefins. Following tertiary processes convert these substances into heavier hydrocarbons and larger polycyclic aromatic hydrocarbons (Li & Suzuki, 2009; Milne & Evans, 1998).

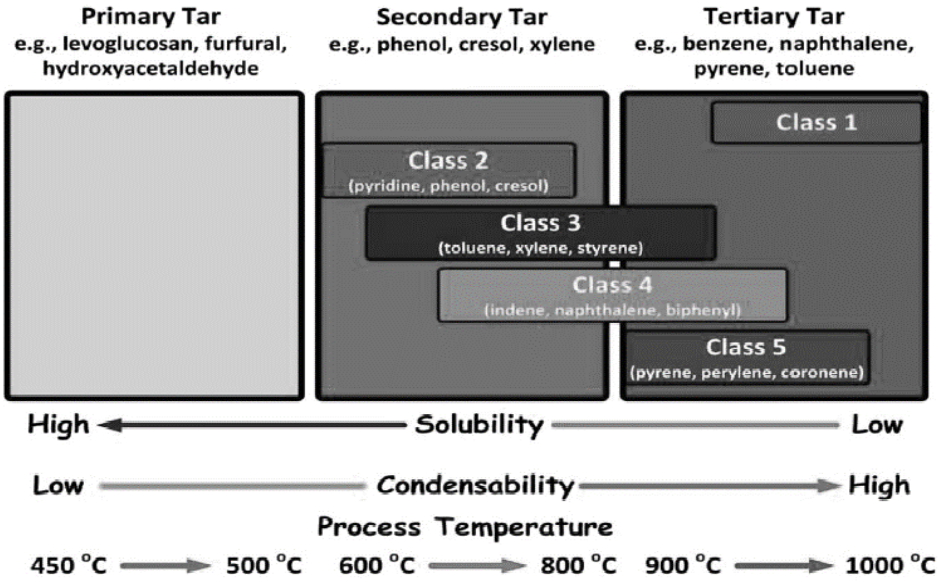

Figure 7. Different groups of tar compounds related to gasification temperature, solubility of tar components and condensation of tar components (Shen, et al., 2016).

Tars are formed from biomass through dehydration, condensation and polymerization reactions. They can be divided into five groups, from the heaviest tar compounds including naphthalene to the most water soluble and lightest group including phenol. In the syngas cleaning and synthesis, tars might cause problems due to decrease in conversion, tars ability to condensate and tars tendency to deactivate catalysts (Stevens, 2001). It is possible for tars to polymerize and to convert into even more complex compounds after gasification in the following process equipment. Additionally, there might occur fouling caused by tar compounds (Li & Suzuki, 2009). To avoid this, concentrations of tar components must be below their condensation points. On the other hand, tar compounds can be cracked into smaller hydrocarbons to produce CO and H_2 (Hamelinck, et al., 2004). Tar production cannot be avoided during gasification and thus tar removal units are needed as a part of the cleaning line (Sikarwar, et al., 2017).

3.2.3 Nitrogen-containing components

The most significant contaminant containing nitrogen in the gasification gas is ammonia. Other possible form of nitrogen in the syngas is hydrogen cyanide (HCN). Ammonia is formed from biomass by primary reactions and from HCN by secondary gas phase reactions (Sikarwar, et al., 2017). Pressurized gasifiers with air as a gasifying agent and feedstock including high amounts of protein produce more ammonia due to reducing environment and higher nitrogen content (Stevens, 2001).

The main motivations for nitrogen removal are regulation and NOx emission issues. NOx emissions are produced when nitrogen-containing gas is burned. Control and removal of nitrogen compounds are not required in all the gasification process systems (Stevens, 2001). Nitrogen can also cause severe catalyst poisoning in some applications (Woolcock & Brown, 2013).

3.2.4 Sulfur

Even small amount of sulfur might be harmful for both the gas cleaning and the synthesis units (Zennaro, et al., 2013; Sikarwar, et al., 2017; Woolcock & Brown, 2013). Main sulfur compounds in the gasification gas are H_2S, carbon disulfide (CS_2), sulfur dioxide (SO_2) and carbonyl sulfide (COS) that are by-products of combustion (Gupta, et al., 2001). The most of the sulfur is in the form of H_2S (Jazbec, et al., 2004). Biomass usually contains less sulfur than coal feedstock (Wakker, et al., 1993; Jazbec, et al., 2004).

Organic sulfur compounds need to be hydrogenated to H_2S before they can be removed by adsorption (Dou, et al., 2002; Zennaro, et al., 2013). Sulfur contaminants may be harmful for some tar cracking catalysts and Fischer-Tropsch synthesis if specific catalysts are used (Zennaro, et al., 2013; Sikarwar, et al., 2017; Woolcock & Brown, 2013). Sulfur can poison Fe, Co and Ni catalysts by forming metal sulfides or it can cause severe corrosion in the process units. In these situations, synthetic gas needs to be cleaned carefully from H_2S and SOx (Stevens, 2001).

4 Combined filtration and pre-reformer

Filtration unit is used to separate phases from each other based on their differences in density, particle size or electric charge (Sutherland, 2008). In hot gasification gas cleaning process, filter unit collects the solid material with the specific size and shape on and inside the filter medium. Different cleaning methods can be applied for these filtration applications such as pulse cleaning. Inlet gas can be pressurized or there can be suction for outlet gas to apply the required pressure drop across the filter medium (Sutherland, 2008; Seville, 1997). This pressure drop affects the permeation behavior of fluid together with particle properties, gas face velocity, cleaning issues, gas composition and filter medium material (Ripperger, et al., 2012; Lupión, et al., 2010).

The hot gas filter does not only remove particulates but it can also be used to collect alkali, chloride and heavy metals. Tars condensate at low temperatures that might complicate the process performance. Otherwise, temperatures higher than 600 °C complicate the filter behavior and cleaning due to the formed sticky cake (Heidenreich, 2013; Simell, et al., 2014). Temperatures between 500-600 °C have found to create the most stable environment for hot gas filtration (Simell, et al., 2014; Hemmer, et al., 2003). As mentioned in the beginning of the thesis, if temperatures below 700 °C are applied for the filtration unit, the total energy efficiency of the process is decreased significantly.

4.1 Filtration parameters

Hot gas cleaning processes favor candle filter configuration consisting of a vertical cylinder vessel filled with filter elements. Cakes form on the outer sides of the filter elements if a typical fluid flow from outside to inside is applied. The filtering element in hot gas applications is usually a smooth tube of porous metal, plastic or ceramic medium with a closed bottom (Seville, 1997).

4.1.1 Pressure drop across the filter medium

Pressure difference across the filter medium is a typical measure for evaluating the filtration behavior. Its value increases during the filtration due to formation of the filter cake and carbon accumulation. There is always some baseline pressure drop that stays across the residual filter cake and filter medium after each cleaning step. If it is constant during the process, the filtration is stable (Simeone, et al., 2011). The total pressure drop across the filter ΔP [Pa] is a sum of the pressure differences across the filter medium and across the cake medium as shown in the equation (22). The pressure drop is illustrated in the Figure 8 for the candle filter (Alonso-Fariñas, et al., 2013).

$$\Delta P = p_1 - p_2 = \Delta p_m + \Delta p_c \quad (22)$$

where p_1 = the gas pressure before the filter [Pa]

p_2 = the gas pressure after the filter [Pa]

Δp_m = the pressure drop across the filter medium [Pa]

Δp_c = the pressure drop across the filter cake [Pa]

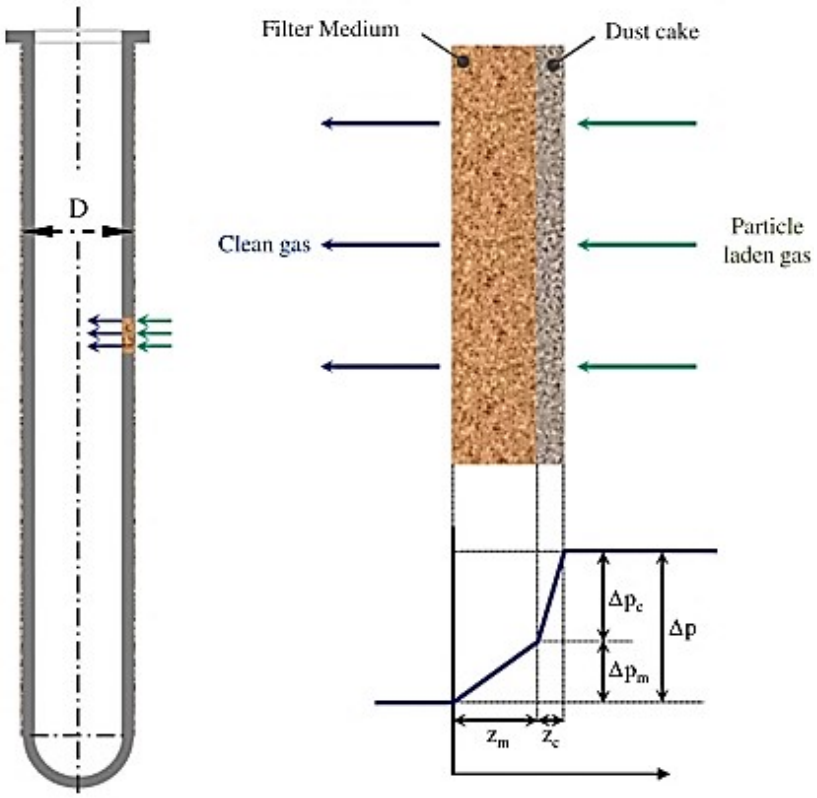

Figure 8. Pressure drop across the candle filter (Alonso-Fariñas, et al., 2013).

Darcy's law (23) can be applied for the fluid flow through the porous medium and it shows the relation between the gas feeding rate, the properties of filter medium and the gas properties at the applied temperature (Ripperger, et al., 2012).

$$Q = -\frac{kA}{\mu} \cdot \frac{dP}{dz} \tag{23}$$

where Q = the volumetric flow rate of the fluid [m^3/s]

k = the specific permeability of the porous medium [m^2]

A = the cross-sectional area of the filter [m^2]

μ = the fluid viscosity [$Pa \cdot s$]

z = the thickness of the porous medium [m]

4.1.2 Gas face velocity

Rate of filtration is usually determined as the gas face velocity *U* [m/s] that is the flow rate of fluid applied per unit area of the filter as shown in the equation 24. This gas velocity takes the surface area of the filter medium into account and thus makes it easier to compare the results between different filtration systems (Ripperger, et al., 2012).

$$U = \frac{Q}{A} \tag{24}$$

The pressure drop can be determined by combining the Darcy's laws (23) for the fluid flow through the filter cake and for the fluid flow through the porous medium. The Darcy's laws and the combined equation are shown in the equations 25, 26 and 27 (Ripperger, et al., 2012).

$$\Delta p_c = \frac{Q}{A} \cdot z_c \cdot \mu \cdot \alpha \tag{25}$$

$$\Delta p_m = \frac{Q}{A} \cdot \mu \cdot \beta \tag{26}$$

$$\Delta P = U \cdot z_c \cdot \mu \cdot \frac{1}{k_C} + U \cdot \mu \cdot \beta \tag{27}$$

where z_c = the thickness of the cake [m]

α = the specific resistance of the cake [m^{-2}]

β = the resistance of the filter medium [m^{-1}]

k_C = the permeability of the filter cake [m^2]

From the equations above, it can be summarized that the pressure drop is affected strongly by the properties of the fluid, the filter medium, formed filter cake and fluid velocity through the filter.

4.1.3 Filter cake properties and cleaning

One of the biggest challenge related to filter process at high temperature is formation of a sticky filter cake. Thus, it is important to evaluate the factors that affect to the formation and properties of the cake (Hurley, et al., 2006). If there is high loading of solids to be removed from the gas, the cake filtration method needs to be applied instead of depth filtration (Jha, et al., 1999). Dust cake has high adhesion and stickiness properties at high temperatures, which can be due to mechanical forces, electrostatic forces, bridging and van der Waals attraction. Bridging occurs due to the particles bonding, sintering or reactions with the filter element (Jha, et al., 1999). It causes instable filtration and finally breaks the filter elements because of the incomplete regeneration (Heidenreich, 2013).

There are many important factors affecting the properties of the formed cake such as particles shape and size, fuel and bed material properties, process conditions, filter material, cake structure and deposition aerodynamics (Hurley, et al., 2006). Dust cake adhesion is determined by the process conditions and the composition and size distribution of the particles in the gas (Chung, et al., 2003). Often it is important to estimate the drag of the gas on the particles (Seville, 1997). Gas viscosity is increased with increase in temperature. This increases also the drag force and thus the filter collection efficiency is decreased (Woolcock & Brown, 2013).

The mean free path is considered as the average distance the fluid travels through the filter medium. The differential pressure of the dust cake depends strongly on the porosity of the cake. If the porosity is decreased for example by compression, the pressure drop of the cake increases. At higher temperatures, the structure and the porosity of the dust cake can change due to the increase of the sticking force or by plastic deformation of the dust particles (Heidenreich, 2013). The dust cake porosity ε_c [-] can be estimated by the equation (28) (Cheng & Tsai, 1998)

$$\varepsilon_c = 1 - \frac{W}{\rho_P z_c} \quad (28)$$

where W = the mass of dust on the filtering medium per unit area [kg/m^2]

ρ_P = the density of particles [kg/m^3]

z_c = the thickness of cake [m].

Hurley et al. (2006) estimates that a cake with a tensile strength over 300 N/m^2 more probably bridges between candles and breaks the filter. On the other hand, if this value is less than 50 N/m^2, there exist problems with cleaning (Hurley, et al., 2006). There are also many other factors affecting these properties such as particle morphology and distribution, the level of moisture and substance concentrations depending on the application. The specific strength (29) can be estimated by the critical thickness index (CTI) [m] that calculates the probability of bridge formation depending on the cake properties. If CTI has the value higher than the distance between two candles next to each other, bridging is likely to take place (Hurley, et al., 2006).

$$\text{CTI} = \frac{\text{tensile strength}}{\text{cake cross-sectional area}} \cdot \frac{\text{cake volume}}{\text{cake weight}} \quad (29)$$

Cleaning properties and efficiency are important characteristics to control filtering process (Seville, 1997). Cleaning has significant effect on the filter process characteristics (Mukhopadhyay, et al., 2016). Usually, cleaning is done by high-pressure pulses of clean air to remove periodically formed dust cake layer (Chung, et al., 2003; Jha, et al., 1999). Temporary dust cake is formed between cleaning processes and can be removed from the filter during the cleaning (Hurley, et al., 2006). The cleaning efficiency $E_{cleaning}$ can be described by the equation (30) (Kim, et al., 2016), in which i represents the time step between cleaning pulses.

$$E_{cleaning} = \frac{\Delta P - \Delta P_{i+1}}{\Delta P - \Delta P_i} \cdot 100\ \% \quad (30)$$

4.2 Reforming of tar compounds

Recent studies have shown that the filter and the filter cake can both take part in the catalytic decomposition reactions of hydrocarbons when the filtration is applied at elevated temperatures above 650 ˚C. Therefore, it is possible to utilize the filter also as a pre-reformer unit (Simell, et al., 2014; Tuomi, et al., 2015). Reforming of tars is conducted at high temperatures due to emission reasons, technical issues and cost reasons (Milne & Evans, 1998). This sets temperature demands for particulates removal step so that energy efficiency of the system remains at the reasonable level (Asadullah, 2014).

Catalytic cracking and reforming by steam can be accomplished at the same temperatures as the gasification (Sikarwar, et al., 2017; Cavattoni & Garbarino, 2017). For the efficient steam reforming, there are multiple catalysts options including natural mineral-based catalysts, metal alkalis and stable metals (Guan, et al., 2016). As mentioned earlier, there might appear catalyst poisoning, coking and sintering when catalytic cracking is applied. In primary reforming, the cleaning is applied already in the gasifier unit. This causes challenges mainly due to difficult scale-up, produced wastes, complicated design of gasifier, difficulties related to cleaning and feedstock demands (Cavattoni & Garbarino, 2017). Challenges of filtration and reforming are discussed in the following chapters.

4.2.1 Sulfur effects on the catalyst behavior

Nickel based catalyst have high potential for tar reforming, but they are disturbed at temperatures around 800 ˚C if sulfur is present in the gas. There is affinity between sulfur and nickel molecules that enables the chemisorption of sulfur on the nickel surfaces (Swisher, et al., 1996). The catalyst deactivates and desulfurization is poor (Rotrupnielsen, 1971; Wang, et al., 2017). Sulfur components in the gas react with nickel catalyst and form non-active surface sulfide Ni-S. (Sato & Fujimoto, 2007; Hepola & Simell, 1997)

Sato et al. 2007 studied the ability of nickel catalyst supported with MgO and CaO to act towards coking and catalyst deactivation due to sulfur poisoning. Good reforming performance was achieved for the naphthalene decomposition (Sato & Fujimoto, 2007).

4.2.2 Carbon accumulation

Temperature and pressure of process affect strongly the carbon formation in the process. For example, increasing pressure increases partial pressures, which might lead to carbon formation on the surfaces. On the other hand, it increases residence time on the filter and thus the conversion of tar decomposition reactions (Sutton, et al., 2001; Devi, et al., 2005). Carbon formation has proved to decrease significantly when temperature is increased from 560 to 800 ˚C (Torres, et al., 2007; Swierczynski, et al., 2007). Especially, nickel catalysts are highly active in tar decomposition but suffer deactivation due to formed carbon that blocks the way to the pores of catalyst (Baker, et al., 1987). Carbon forms as a product of incomplete reforming reactions when relatively high amounts of tars are present in the gas (Nacken, et al., 2009; Swierczynski, et al., 2007). Precious metal catalysts have shown better resistance towards carbon formation probably due to their catalytic activity towards carbon gasification (Kaisalo, et al., 2015). Nickel/dolomite catalysts have also shown good resistance towards carbon deposition (Srinakruang, et al., 2005).

The presence of steam in higher amounts can enhance the catalyst activity by removing carbon through steam reforming (Sutton, et al., 2001). The effect of catalyst support, such as MgO, is studied widely and shown that it can be used to control the balance between reactions of carbon formation (Baker, et al., 1987; Nacken, et al., 2009). Garcia et al. 2000 studied the possibilities to utilize cobalt and chromium additives to disturb the coke producing reactions (Garcia, et al., 2000). It is possible to reduce carbon accumulation by dividing the reforming process into more than one stages and by utilizing different catalyst in the pre-reformer unit. Simell et al. 2015 proposed that some noble metal catalyst would be applied in the pre-reformer unit

and a metal catalyst would be used in the next stage (Simell, et al., 2015). Dolomite bed has been studied to act towards carbon formation when added as a guard for nickel catalyst (Sutton, et al., 2001). Carbon formed during the filtering process can be removed by burning the reactor (Torres, et al., 2007).

5 Filter technologies and equipment

Cleaning of the gasification gas involves challenges according to the varied feedstock, catalysts deactivation, tough process conditions and required high purity (Simell, et al., 2014; Heidenreich, 2013). Filter processes are preferred for the hot gas applications due to their simplicity and good resistance for high temperature. (Heidenreich, 2013) Severe pressure drop might follow by the fouling of tars and particulates making process unprofitable (Sansaniwal, et al., 2017). When temperatures are high, the cake properties can also change due to chemical solid phase reactions in the dust or reactions between dust and gas (Heidenreich, 2013). There are cold gas cleanup technologies for cleaning the syngas to reasonable level, but cooling of the gas decreases the overall efficiency and makes the process unprofitable as discussed in the previous chapter. Demand for suitable and profitable hot gas cleaning equipment is high (Abdoulmoumine, et al., 2015). This chapter gives some general overview on the filtering processes and materials developed for hot gas cleaning applications. First, promising filter materials are discussed and then the report focus on the catalyst solutions in more details.

5.1 Filter materials

There are many different filter materials proposed for hot gas filtration. Conventional fabric materials do not work for these applications due to their fragility at high temperatures and pressures. There exist both ceramic and metal filters that have good resistance and stability at challenging process conditions. Rigid filters are the most suitable option due to their resistance for high temperatures and corrosion with great collection efficiencies (Mukhopadhyay, et al., 2016; Seville, 1997). There is a need for high chemical stability against reactive gas species including hydrogen sulfide (Heidenreich, 2013). Most of the experiments have been done in laboratory scale with ceramic hot gas filters (Simell, et al., 2014; Simeone, et al., 2013; Nacken, et al., 2010).

Usually the experiments studying gasification gas cleaning equipment utilize dust-free gas including naphthalene, phenol, toluene or benzene to represent tar compounds in the gas. Naphthalene represents often the most problematic tar compounds (Abdoulmoumine, et al., 2015).

5.1.1 Ceramic filters

Most of the ceramic filters currently available for hot gas filtration are made of a thin outer layer consisting of silicon carbide or alumina silicate which is connected to the main body composed of course-ground silicon carbide (SiC). The ceramic filters show very good filtration efficiency at temperatures up to 800 ˚C (Cummer & Brown, 2002; de Jong, et al., 2003; Sharma, et al., 2008). Cracks can appear after a thermal shock caused by pulse cleaning in which the cleaning gas, for example air, flows counter-currently through the filter system (de Jong, et al., 2003). Cracks can also appear after explosions inside the candles due to the combination of dust and flammable gas (Sharma, et al., 2008). Ceramic filter prefer high-pressure cleaning due to the large pressure drop across the filter (Hasler & Nussbaumer, 1999).

Ceramic filters can have either high-density or low-density structures, of which suitability depends on the application. High-density structures with porosities around 40 % consist of sintered grains made of for example silicon carbide or alumina. Typical low-density ceramic filters consist of alumina silicate fibers with porosities up to 90 %. High-density ceramics are mechanically stable and tolerate better back cleaning pulses than ceramic materials with lower densities (Heidenreich, 2013). The collection efficiency of these elements is very high and they have good ability to filtrate even smaller than micron size particles (Heidenreich, et al., 2002; Cummer & Brown, 2002).

Although there are multiple ceramic candle filters, which can efficiently remove particles from the gas, they cannot remove tar components and other contaminants. Under hot gas filtration, the tar components are in the gas phase and without reforming reactions they flow through the filter medium (Asadullah, 2014). Additionally, ceramic filters may be too brittle and prone to break down when

temperature or load is changed (Jha, et al., 1999). Therefore, cyclone and ceramic filter cannot be used for complete cleaning of gas but they can be used in combination with other methods for gas cleaning (Asadullah, 2014).

5.1.2 Metallic filters

Metal filters are often restricted in hot gas cleaning applications due to possible metal sintering and corrosion (Stevens, 2001). On the other hand, they can offer the required strength at high temperatures, corrosion resistance and toughness for varying process conditions when designed correctly (Jha, et al., 1999). As mentioned earlier, there are several problems related to tars and high temperatures when ceramic filters are used. These problems have been tried to overcome by metal filter materials. There exist metals that can be used at temperatures as high as 1000 ˚C with good filtration efficiencies. Anyway, most of the experiments with metal filters are accomplished at temperatures between 400-700 ˚C (Cummer & Brown, 2002; Hofmann, et al., 2008; Ghidossi, et al., 2009).

Different cleaning and regeneration solutions have been developed for enhancing the metal filter systems. Metal filters can perform with complete regeneration by sulfuric acid backwash system, but this needs to be accomplished at room temperature (Ghidossi, et al., 2009). Another option is to use the clogged filter in an oven with air circulation at 900 ˚C for some specific time to achieve complete oxidation of the particles to be removed. This option, leads often to incomplete regeneration and the process is time consuming (Villot, et al., 2012; Ghidossi, et al., 2009).

Different metal alloys and steel grades are applied for filtration units. Stainless steel filter materials are usually used only at temperatures below 420 ˚C and high temperature steels are proved to work efficiently below 650 ˚C. Metal filter raw materials are typically fibre metals, metal fabrics or metal powders sintered at high temperatures. Fibre medium are produced from short fine metal fibres and sintered in hydrogen or under vacuum. Powder medium with porosity between 20-40 % are manufactured by pressing followed by sintering under vacuum or in hydrogen

(Heidenreich, 2013). Sintering increases the survival time of the material, enhance the corrosion resistance and simplifies the cleaning. The most significant difference when compared to ceramic materials is strength and toughness achieved by sintering. The main restrictive property at high temperatures with metals is the sulfurizing caused by sulfur present in the gas (Jha, et al., 1999).

Main problems are related to the oxidation and corrosion that increase volume and plug the medium pores. Only few special metal alloys can handle existing sulfur and chlorides. Examples of these are Inconel 600, Monel or Hastelloy X (Tortorelli, et al., 1999; Heidenreich, 2013). Filter surface can be protected and maintained clean by a protective layer. Metal filters can be coated with alumina oxides for protection (Sharma, et al., 2010; Kim, et al., 2008). By heat treatment at about 1000 ˚C under oxidizing atmosphere, aluminum moves to the surface and generates a protection surface. This protection layer is compact and very corrosion resistant. The maximal operating temperature of these elements is around 1000 ˚C (Succi, et al., 2008; Heidenreich, 2013). Oxide layers have good tolerance against material corrosion at least at temperatures below 800 ˚C (Heidenreich, 2013; Guan, et al., 2008).

5.2 Catalysts

Gas filtration of particulates and catalytic pre-reforming of tars can be combined by using a catalytic filter medium (Nacken, et al., 2012). Catalyst can be integrated on the pore walls of the filter candle, by the fixed bed design in which catalyst is integrated as fixed bed into the candle filter (Nacken, et al., 2009; Nacken, et al., 2010; Nacken, et al., 2012) or as a thin layer on the filter medium surface (O'Neill, et al., 2015). Catalytic layer designs are simpler to apply, to scale-up and to produce than more complex fixed bed designs but the fixed bed designs are noticed to have higher catalytic activity towards tars decomposition in many candle filter applications (Nacken, et al., 2012; Villot, et al., 2012).

5.2.1 Catalyst options

Catalysts from mineral options to nickel-based catalysts are found to be efficient for reforming tars at temperatures between 800-1000 ˚C with conversions higher than 90 % (Simell, et al., 2014). Char, dolomite, olivine, alkaline metals and Ni-based catalysts are inexpensive options for reforming catalysts (Cavattoni & Garbarino, 2017). Noble metal catalysts are efficient tar decomposition catalysts but more expensive when compared to other options. (Tomishige, et al., 2003; Li, et al., 2015) Main challenges in these applications are contamination, deactivation and sulfur poisoning. If alkali catalysts are used the alkali oxides may volatilize and cause harm in the following process units (Cavattoni & Garbarino, 2017). Catalyst may deactivate by coke deposition, sulfur can poison it or ashes can contaminate it (Cavattoni & Garbarino, 2017; Simell, et al., 2014). Challenges to find the suitable catalyst for tar reforming are caused by the complexity of occurring reactions and existing tar compounds in the gasification gas. With experiments of model, tar compounds, only half of the picture of process performance can be modeled (Guan, et al., 2016).

Natural minerals can be applied both as preliminary or secondary catalysts in biomass gasification applications (Guan, et al., 2016). The calcined olivine and dolomite have both shown good activity towards gasification reactions and towards decomposition of tar compounds (Hu, et al., 2006). The main advantages of these materials are their price, good activity and non-toxicity (Sutton, et al., 2001; Constantinou, et al., 2010). Dolomite is the most effective catalyst of the natural minerals but it produces more particulates during gasification than olivine (Aznar, et al., 1998). Furthermore, there occurs deactivation because of the carbon deposition and abrasion. Dolomite cannot reform methane (Sutton, et al., 2001). It has been shown that CaO is more catalytically active component than MgO towards tar decomposition (Simell, et al., 1996). Zeolite has potential to work as a good support for catalysts due to its high stability and strength (Guan, et al., 2016). Tuomi et al. 2015 studied the hot gas filtration performance and noticed that at 800˚C, ceramic candle filter unit behaved as a pre-reformer and decomposed 50 wt-% of tar components due to the long residence time,

catalytic activity of residual biomass char and catalytic nature of dolomite bed material (Tuomi, et al., 2015).

Alkali metal catalysts such as potassium, sodium and lithium have also been studied especially as primary catalysts in the gasifier (Mudge, et al., 1987). They help to decompose tar components and to increase gasification rate (Mitsuoka, et al., 2011; Kuchonthara, et al., 2008). Recovery of catalyst is complicated and catalyst might evaporate during the reactions. Some biomass ash contains high amounts of alkali metals and can thus perform as a catalyst. If alkali components in biomass could be utilized in tar reforming, also problems related to handling the ash in gasification could be overcome (Hognon, et al., 2014). Alkali metal catalysts such as potassium carbonate supported on alumina are not so sensitive towards carbon formation when used as secondary catalysts but also decomposition conversions of tars seem to be lower (Sutton, et al., 2001; Mudge, et al., 1987).

Nickel catalysts can effectively decompose tars by steam reforming, decrease NOx emissions and increase both WGSR (2) and methane reforming (10) reaction rates (Aznar, et al., 1998; Wang, et al., 2017). There are several studies related to the different supports and promoters added to enhance nickel catalysts performance towards sulfur deactivation and coking (Ma, et al., 2005). Catalyst including Ni, Al_2O_3 and MgO have given naphthalene conversions above 99 % even with present of sulfur both at 800 °C with silicon carbide filter medium (Nacken, et al., 2012) and at 900 °C with porous alumina filter medium (Ma, et al., 2005). Silicon carbide based filter elements with MgO - Al_2O_3 supported Ni catalyst have shown 99 % conversion for naphthalene at 800 °C with 2.5 cm/s gas superficial velocity and with present of sulfur (Nacken, et al., 2012). Deactivation can take place due to carbon deposition or nickel particle growth (Sutton, et al., 2001; Wang, et al., 2017). One advantage of nickel catalysts is their ability to enhance conversion of ammonia (Leppälahti, et al., 1991). In some experiments, Co/MgO pre-calcined catalysts have shown better activity towards naphthalene decomposition than NiO-MgO catalysts, but this needs to be studied more to see their real potential (Furusawa & Tsutsumi, 2005).

Noble metal catalyst are proved to be effective catalysts in tar reforming processes with high activity and stability. The only problem seems to be their high price (Guan, et al., 2016). Noble metal catalyst with zirconia support has given good results for hot gasification gas applications. Rhodium catalyst seems to be the most catalytically active option with resistance towards carbonization of reactor and toward sulfur poisoning (Rönkkönen, et al., 2010). Rh/m-ZrO_2 catalyst performed complete toluene and naphthalene conversions at 900 ˚C (Rönkkönen, et al., 2011).

5.2.2 ALD coatings

In the experiments of this thesis, Atomic Layer Deposition (ALD) coating technique was used to apply nickel catalyst on the metal filter medium. This means, that the thin-film catalyst coating is produced by the chemical self-limiting gas phase reactions on the substrate surface. Usually, a metal reactant and an oxygen source are used to produce the catalyst coating of desired thickness (O'Neill, et al., 2015; Marichy, et al., 2012). The technique enables to produce precise structures at atomic level with improved activity and stability of catalysts (Johnson, et al., 2014).

The catalytic layers are formed through the cycles and the desired thickness is achieved by optimized process conditions, pulsing times and number of cycles (Miikkulainen, et al., 2013). In one cycle, first, one of the reactants is pulsed to the filter medium where it reacts with the surface. The purge gas removes both unreacted reactant and by-products before the second reactant is added to the surface. After this, the surface is purged again and the cycle is ended (Marichy, et al., 2012). When a high vapor pressure metal precursor such as $Ni(tmhd)_2$ (bis(2,2,6,6-tetramethyl-3,5-heptanedionato)nickel(II)) is used, precursor reacts with the surface in the first half-reaction so that reactive ligands of precursor react with surface active sites. In the second part reactions, oxygen reactant such as ozone deposits oxides or reducing agent and removes remaining ligands of the metal precursor regenerating the active sites (O'Neill, et al., 2015; Seim, et al., 1997).

5.3 Filter modifications and configurations

Performance of the separation unit can be enhanced by modifying the structure, medium, support, promoter or catalyst of the filter (Heidenreich, 2013). Additionally, the cleaning system of the filter can be modified. For example, the coupled pressure pulse (CPP) cleaning system can ensure regeneration of the candle filter and efficiency of particle removal despite the blocking of the filter by the cake (Mai, et al., 2002; Simeone, et al., 2013). Each candle is in connection with the re-cleaning gas reservoir through a valve and pressurized gas is pulsed from inside to outside of the filter element. Nitrogen is used to purify candle filters with reverse pulse cleaning (Simeone, et al., 2011).

The preferred geometry for hot gas filter elements is the form of a candle, which is closed at one end as already mentioned. The cake is typically built up on the outside surface of the candles and the gas flows from outside to inside. In addition, other flow directions and different tube model filters exist but they are more seldom used in these applications. Some geometries have been tested aiming to achieve larger densities for the filtration areas (Heidenreich, 2013). One example is monolith filters with a honeycomb structure of a parallel set of cells. The feedstock gas flows from the open end of the upstream cell through the wall to the downstream cell and exits from the opposite open end of that cell. The problems arise if the upstream cell is blocked due to its difficult cleaning by back pulse (Heidenreich, 2013; Pitcher , 1982).

By making the membrane thin, the differential pressure of the filter element is limited. An optimum is to have a very thin layer so that surface filtration is achieved. Penetration of particles into the support structure is prevented and the element can be effectively regenerated by back pulsing. This is an advantage with regard to the long-term behavior of the filter elements and their lifetime (Seville, 1997; Heidenreich, 2013). The pore size and the size distribution can be adjusted by selecting the right grain sizes. Furthermore, an option to adjust the pore size and porosity is to add pore-forming materials, which burn out during the sintering process, such as sawdust (Heidenreich, 2013).

Catalytic filter candle called DeTar filter is one example of the equipment developed to combine particulate filtration and tar reforming in one process unit (Nacken , et al., 2015). Nacken et al. (2012) tested a novel catalytic filter with this structure and with activated ceramic foams on the hollow-cylindrical space of filter element. This filter design is shown in the Figure 9. They used catalytic layer of $MgO\text{-}Al_2O_3$ -NiO and compared SiC based ceramic foam to Al_2O_3 based foam at process temperatures between 800-850 ˚C. Test results showed that naphthalene conversion of 98 % can be achieved with Al_2O_3 based foam filter in the presence of H_2S with superficial velocity of 2 cm/s at temperatures around 850 ˚C. The conversion of naphthalene was evaluated to be 18 % higher than it was with the SiC candles at same conditions but without the integrated catalytic foam of the higher rigidity (Nacken, et al., 2012). The Al_2O_3 based foam filter is also tested at the bench-scale with results of 94 % for naphthalene conversion with 4100 ppmv H_2S content, 2 cm/s filtration velocity and at temperature around 850 ˚C (Nacken , et al., 2015).

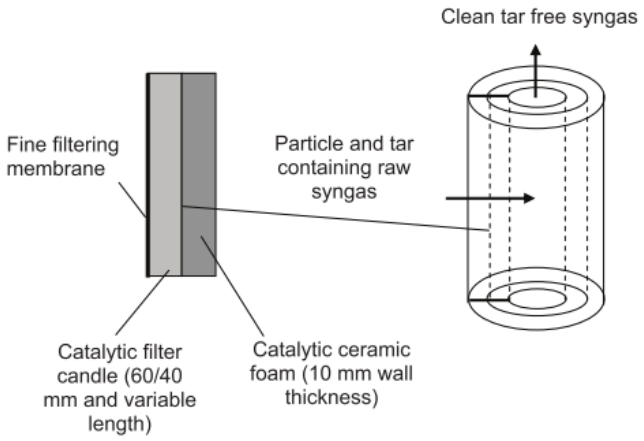

Figure 9. Hot gas filter coated with activated ceramic foams (Nacken, et al., 2012).

Simeone et al. (2011, 2013) have performed filtration tests at temperatures around 800 °C with atmospheric CFB steam/O_2 gasifier system with magnesite and biomass feedstock wood. The filter included thin mullite grain membrane ($3Al_2O_3\ 2SiO_2$) and silicon carbide support. The results showed that there was fast increase in pressure drop caused by the penetration of fine ash into the filter medium followed by pores

clogging. At temperatures around 600 °C, these kind of problems did not exist (Simeone, et al., 2013; Simeone, et al., 2011).

D'Orazio et al. (2015) made experiments with three different ceramic filters integrated to the freeboard of the steam gasifier. The non-catalytic candle with new support, filter candle with catalytic layer and filter candle with integrated catalytic foam system were tested. The best results were achieved with the foam catalyst system when the tar content, water conversion, hydrogen production and ammonia decomposition were considered. The non-catalytic system showed the highest pressure drops. Hot gas filter candles were made of Al_2O_3 with MgO - NiO catalyst layers and MgO-Al_2O_3-NiO as catalytic foam (D'Orazio, et al., 2015). Also Rapagnà et al. (2009) tested ceramic candle filters in a gasifier freeboard with good test results for catalyst system with increased gas yield, higher hydrogen concentration and decreased tar amounts. They used a silicon carbide medium with a mullite outer surface as a filter supported by MgO - Al_2O_3 nickel-catalyst (Rapagnà , et al., 2009). As mentioned earlier, scale-up is one major challenge in the systems of integrated filter and gasifier systems. Additionally, there is a need for more studies for the long-term tests and filter cleaning efficiencies (D'Orazio, et al., 2015; Rapagnà , et al., 2009). The simplified gasifier system with integrated candle filter unit modified from the (Rapagnà , et al., 2009) is shown in the Figure 10.

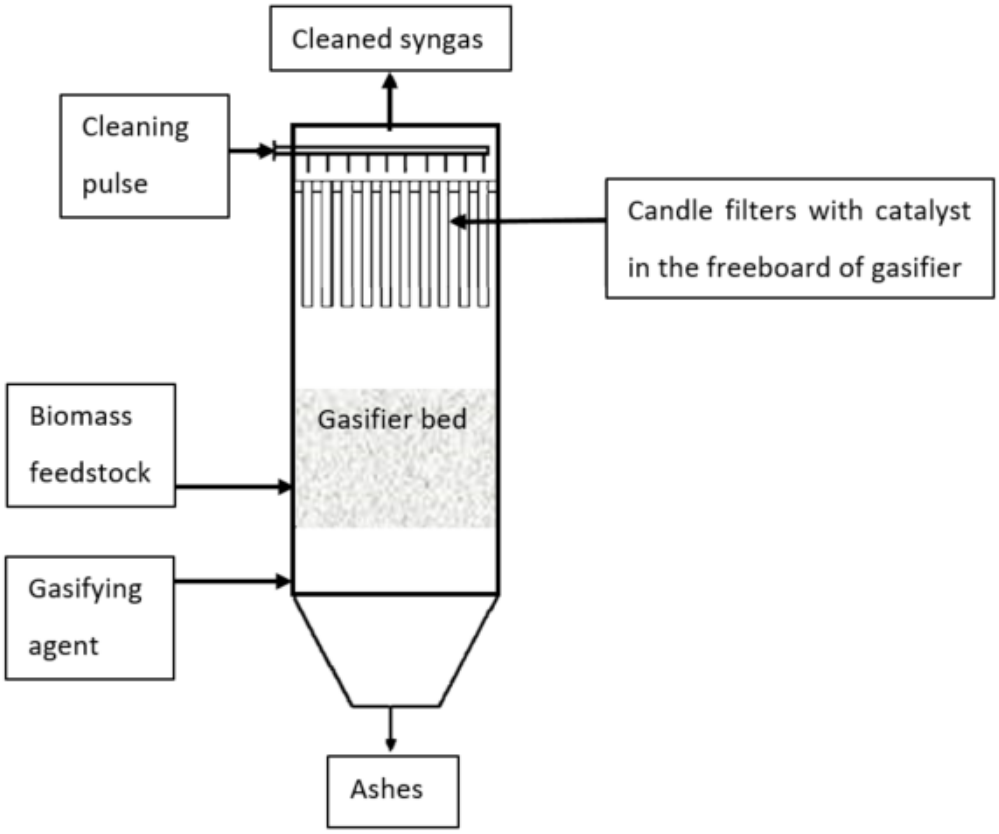

Figure 10. Gasifier unit integrated with the candle filter unit. Figure modified from the (Rapagnà , et al., 2009).

6 Experimental

For the experimental part of the thesis, the experiments were carried out in the laboratory at VTT Technical Research Center of Finland. The aim was to study the new filter system for gas cleaning purpose. Process conditions, gas feeding velocities and filter medium configurations were varied to study their effects on the decomposition of tar components and on the filter performance.

6.1 Experimental gas composition

Composition of the feeding gas was maintained constant during all the experiments. One experiment was carried out in the absence of H_2S to see its effect on the catalyst performance. The wet gas composition is shown in the Table 5. As can be seen from the table, the main substances in the gas were H_2, CO, CO_2 and CH_4. Additionally, smaller amounts of C_2H_4, H_2S and tar components were added to model the actual gasification gas composition. The rest of the gas was nitrogen. Purities and producers of each components can be found in the Appendix 2. The content of ion-exchanged water in the feed was 44.3 vol-%. Effect of ammonia on the filtration process was not studied in these experiments.

Table 5. Composition of the wet gasification gas fed to the filter unit.

Wet gasification gas	
Component	Content (vol-%)
CO	10.7
CO_2	15.5
H_2	22.7
CH_4	2.8
N_2	2.0
C_2H_4	1.7
H_2O	44.3
Component	Content (vol-ppm)
H_2S	60
Tars	3643

Tar compounds present in the gasification gas were demonstrated with the model tar mixture including naphthalene, toluene and benzene. Amounts of tar components are shown in the Table 6. Naphthalene is the most essential component in the tar mixture due to its problematic nature as mentioned in the literature part of the thesis. In reality, there is a wide range of different tar components, which makes the process even more complicated. Benzene is usually a relatively easy component to remove. Toluene represented monoaromatic and naphthalene polyaromatic tar components in the gasification gas.

Table 6. Composition of the tar solution and their content in the wet gasification gas.

Component	Content in tar solution (w-%)	Content in wet gasification gas (vol-ppm)
Benzene, C_6H_6	43	1956
Toluene, C_7H_8	50	1434
Naphthalene, $C_{10}H_8$	7	253

6.2 Experimental setup

The test rig comprised feeding, reactor and product analysis sections. Water was evaporated before it was combined with tars. All the components were combined and heated up to 200 ˚C before they were fed to the reactor. After the reactor, small part of the wet product gas was directed to the gas chromatograph. The rest of the gas flowed to the condensation unit, which included both propane and water flasks submerged in the ice. From the condensation unit, the dry gas without tars and water flowed to the gas analyzer. Experimental setup of the reactor is shown in the Appendix 1. The simplified process flow diagram of the system is shown in the Figure 11.

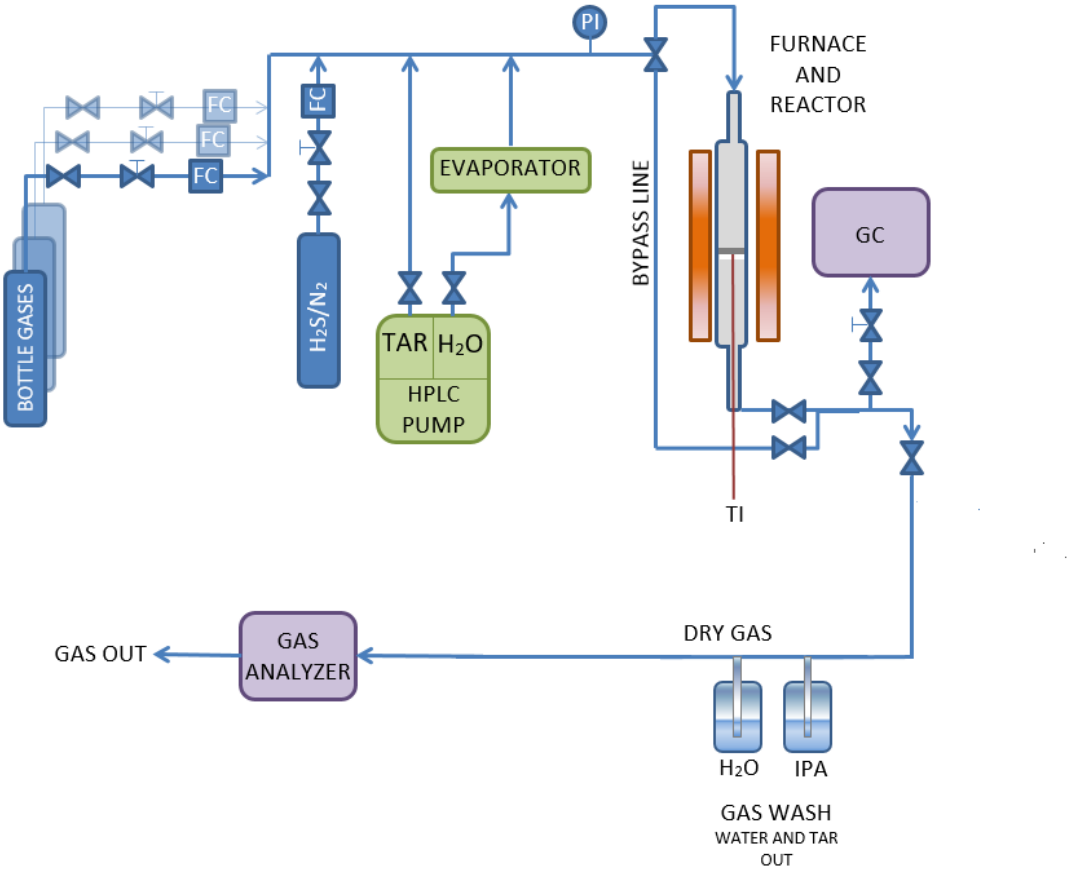

Figure 11. The experimental setup of pressurized reactor system (Modified from the drawing made by Mari-Leena Koskinen-Soivi, VTT Technical Research Center of Finland).

The gas mixture was fed to the reactor at 200 ˚C and at atmospheric pressure. The feeding gas flow was controlled with separate mass flow meters of each component and the high-pressure liquid chromatography pumps (Agilent Technologies G1310A Iso Pumps) were used to control the feeds of water and tar mixture. Used mass flow meters are listed in the Table 1 of the Appendix 2. Gas analysis and operational ranges of the flow controllers limited the gas flow and thus only flows above 0.75 l/min could be applied. The gas was fed with velocities of 1.0 or 1.5 l/min in most of the experiments.

The reactor used in the experiments can be seen in the Figure 12. The oven was 47 cm long and the reactor inside it consisted of two sections. The reactor tube included a sinter on which the filter was placed. Thermoelement measured the temperature

inside the reactor from the upper side of the sinter, which was right under the filter medium, as shown in the Figure 12. Gas flowed from above through the reactor tube. Diameter of the reactor was 2.6 cm at the point in which the sinter was placed. The pressurized plug flow reactor was placed inside the three-zone furnace and had a bypassing line.

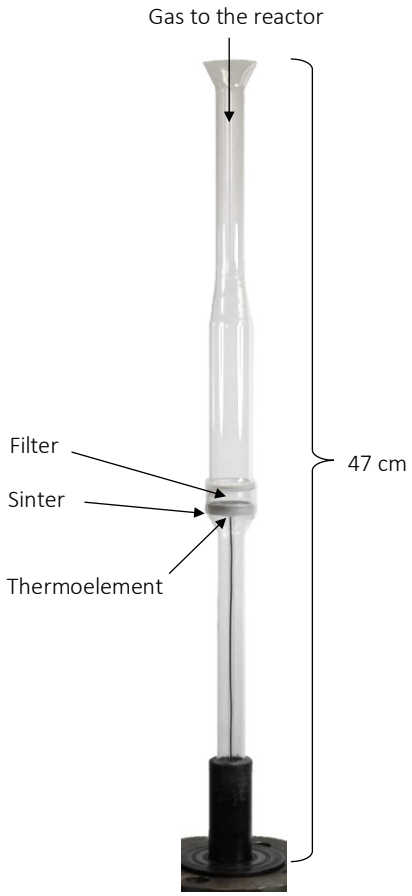

Figure 12. The two-section pressurized tube reactor and the furnace system.

Reactor temperatures of 700, 800 and 900 ˚C were studied. The outlet of the reactor was kept at 200 ˚C before condensation and the line to the gas chromatograph was kept at 180 ˚C. Pressures between 1-5 bar were tested. Pressure was controlled based on the pressure at the inlet of reactor. The pressure drop across the filter was measured as the difference between the inlet and outlet pressures. All the experiments and their process conditions are listed in the Appendix 3

6.3 Filters and catalysts

Metal filters manufactured by GKN Sinter Metals Filters were used in the experiments. These filters were 3 mm thick and had diameters of 25.4 mm. The pore sizes were between 75-300 µm. The filters were both sintered and oxidized. They were made of stainless steel (AISI 316L) and in some experiment coated with ALD nickel coatings. The list of the used filters can be found in the Table 2 of the Appendix 3. The filters were set inside the reactor with the help of quartz wool as shown in the Figure 13. Quartz wool prevented the by-pass flow. Flow through and pressure drop over the filter medium were studied with different nitrogen flowrates and varying temperatures before the actual experiments.

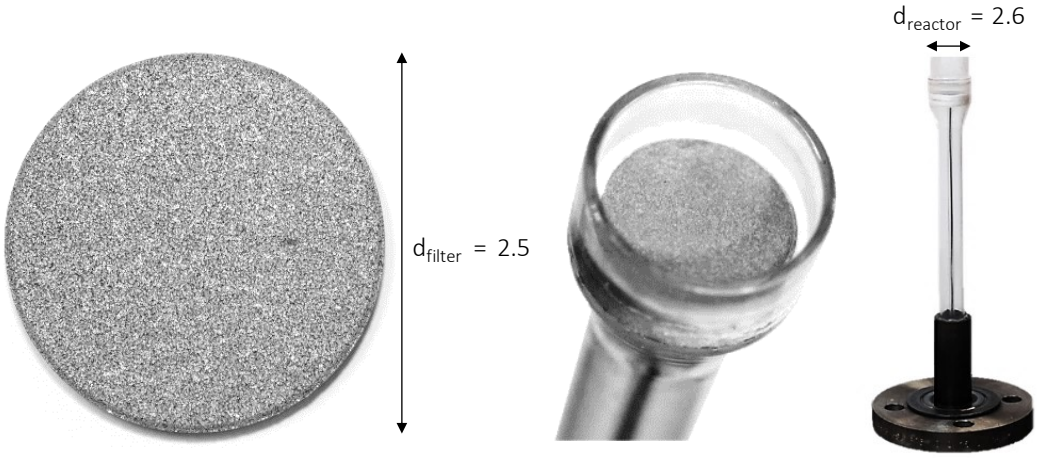

Figure 13. Configuration of the used metal filters.

Nickel catalyst was added on top of the filter medium with the ALD technique, which was introduced in the chapter 5.2.2. Different amounts of NiO coatings were tested in the range of 13-65 nm. Additionally, in some experiments Al_2O_3 was tested to add under the nickel coating as a supportive and protective material. Its potential to support was also tested by applying it on the surface of the nickel coating. ALD coated filters were activated by reducing them 1 hour at 800 ˚C to convert NiO to Ni at atmospheric pressure in the beginning of the experiments. This was done by feeding the mixture of 50 vol-% hydrogen and 50 vol-% nitrogen with gas flow of 1 l/min. ALD coatings were made at temperatures of 225 ˚C. Bis(2,2,6,6-tetramethyl-3,5-heptanedionato)nickel(II) and O_3 were used as precursors for NiO coatings. Alumina support was produced from trimethylaluminum (TMA) and H_2O precursors.

6.4 Methods and technique

The pressure test and cleaning of the reactor line were accomplished with 1.5 l/min purge nitrogen flow before each experiment. First, the gas mixture flowed through the by-pass line until the compositions of the gas components were stabilized and pressure was set to the right value. Then the gas mixture was turned to flow through the reactor. Due to carbonization of the reactor, oxidation was needed after each experiment.

Experiments with empty reactor without a filter at temperatures of 700, 800 and 900 ˚C showed that there was no increase in the pressure drop across the sinter and naphthalene concentrations remained constant with all the temperatures. Some of the toluene and ethylene decomposed to form benzene and methane at 900 ˚C due to thermal degradation reactions. At lower temperatures, these thermal decomposition reactions did not occur in significant amounts.

Temperatures between 700-900 ˚C and pressures 1-5 bar were studied. Experiments were started either at temperature of 700 ˚C or 800 ˚C. Temperature was increased during the experiment so that essential temperatures were studied and experiment was ended after the highest temperature setup. The experiments were conducted one pressure set point at a time.

6.4.1 Product analysis

Before the condensation equipment, small part of the gas was directed to the gas chromatograph (GC) for gas analysis. The composition of tars, C_2H_4 and methane in the wet product gas were measured by the online gas chromatograph with flame ionization detector (FID). Chromatograph (Agilent 7890A GC) utilized helium as a carrier gas. Different components in the gas interact with the liquid and elute at different retention times. Chromatograph enabled to measure light hydrocarbons including methane and ethylene and heavier hydrocarbons including benzene, toluene and naphthalene in the sample gas. In the chromatograph, gas sample was directed through the 6-way valve to the HP-5 column. From the HP-5, gas continued to the GS-GASPRO column. After lighter hydrocarbons reached the GS-GASPRO, Dean Switch was turned off so that heavier hydrocarbons reached only the HP-5 column. From the columns, heavier hydrocarbons flowed to the FRONT-detector and lighter to the BACK-detector (Agilent Technologies, Inc., 2010).

The gas from the condensation unit was directed to the gas analyzer. The Sick Maihak type S710 online gas analyzer was used to measure the composition of methane, hydrogen, carbon monoxide, carbon dioxide and oxygen in the dry product gas. Gas

analyzer unit included separate analyzers for oxygen and for carbon monoxide, carbon dioxide, methane and hydrogen. The sampling system had a pump for samples and a removal unit to remove condense water to the washing flask. Analyzer was calibrated at least every other week (Maihak AG, Werner, 2000).

The H_2S and COS contents were not measured in these experiments. In addition, the water and nitrogen contents of the product gas stayed unspecified, but they were estimated in the mass balance calculations. The gas chromatography results were mainly studied to get the conversions for tar components, methane and ethylene. Thus, amounts of other hydrocarbons present in the gas were not concentrated in more detail.

6.4.2 Calculation methods

Inlet and outlet gas compositions were calculated from the average values obtained during the sampling time. Hydrocarbon concentrations were measured by the gas chromatograph and these results were used to calculate the conversions of naphthalene, toluene, ethylene, methane and benzene in the system, by utilizing the following equation (31). Yields for the CO, H_2O, CO_2, CH_4 and H_2 were calculated with the equation (32).

$$X_i = \frac{F_{i,in} - F_{i,out}}{F_{i,in}} \cdot 100\% \quad (31)$$

where X_i = conversion of the component i [%]

$F_{i,in}$, $F_{i,out}$ = molar flow before and after reactor [mol/s]

$$Y_i = \frac{F_{i,out} - F_{i,in}}{F_{i,out}} \cdot 100\% \quad (32)$$

where Y_i = yield of the component i [%]

Molar flows were calculated based on mass balances at steady states. All the achieved conversions and yields are shown in the Appendix 4. One calculation excel example for the system mass balance is shown in the Appendix 5. The total volume flow rate of the

product gas was estimated based on the carbon and hydrogen balances. Water amount in the product gas was estimated based on the hydrogen and oxygen molar balances. The amount of nitrogen was assumed to stay constant because it was not consumed in the reactions. The equation (33) was used to calculate the wet gas composition based on the dry gas composition results from the gas analyzer.

$$vol\text{-}\%_{i,wet} = \frac{vol\text{-}\%_{i,dry} \cdot Q_{dry}}{Q_{wet}} \quad (33)$$

where $vol\text{-}\%_{i,wet}, vol\text{-}\%_{i,dry}$= volumetric composition of the component [%] in wet gas and in dry gas

Q_{dry}, Q_{wet} = volumetric flowrate of the dry gas and wet gas [m^3/s]

Product gas was assumed to follow the ideal gas rule, in which the amount of gas component can be calculated based on the equations (34) and (35).

$$n_i = \frac{m_i}{M_i} \quad (34)$$

where n_i = number of moles [mol]

m_i = mass of the component i [g]

M_i = molar mass of the component i [g/mol]

$$n_i = \frac{V_i}{V_m} \quad (35)$$

where V_i = volume of the component i [m^3]

V_m = molar volume of the component [m^3/mol]

Gas face velocity and gas hourly space velocity (GHSV) [h^{-1}] are typical values used in the catalyst applications to show the relation between the fluid velocity and process system. These values were calculated with the equations (24) and (36).

$$GHSV = \frac{Q}{V_{reactor}} \quad (36)$$

The amounts of carbon formed on the filter surface and on the reactor walls were estimated by weighting the filter medium before and after the experiments.

Additionally, the gas analyzer recorded the amounts of carbon monoxide and carbon dioxide produced during the reactor oxidation. These volume fractions were used to calculate the molar amount of carbon that was released during the oxidation.

The error related to the pressure controller inside the reactor was calculated with the equations (37).

$$Error,\ P\ (\%) = \frac{P_{set\ point} - P_{measured}}{P_{set\ point}} \cdot 100\ \% \tag{37}$$

where $P_{set\ point}$ = setup pressure for the reactor [Pa]

$P_{measured}$ = measured pressure inside the reactor [Pa]

7 Results and discussion

This chapter concentrates to introduce the most important results achieved from the experiments. Results are evaluated based on their reliability and they are compared to the results found in the literature. First, the effect of process conditions on the pre-reformer and filtering performances was studied and after that, different surface velocities and filter configurations were tested.

7.1 Different pressures

Experiments at 1 bar and 3 bar did not result in high level naphthalene decomposition. Only conversions of naphthalene below 10 % were achieved. The main results based on the experiments at 1 bar are shown in the Figure 14.

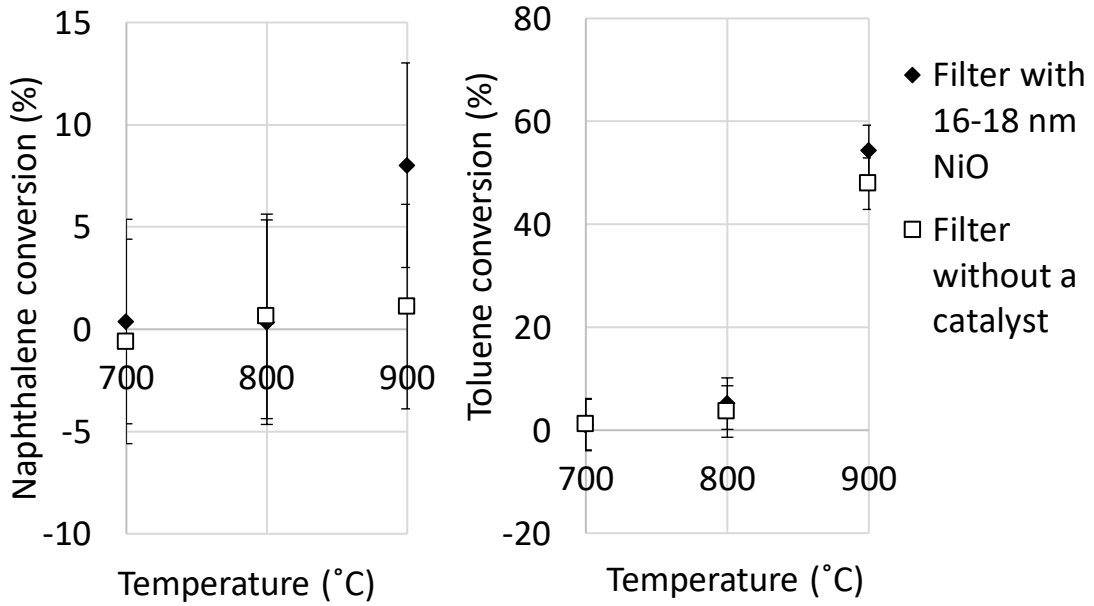

Figure 14. Conversions of naphthalene and toluene at 1 bar as a function of temperature with 1.5 l/min gas feed.

From the Figure 14, it can be seen that at 1 bar there was no decomposition of naphthalene without a nickel catalyst. Also with a nickel catalyst, only conversions

below 9 % were achieved for naphthalene at 900 °C. At 700 ˚C and at 800 ˚C, catalyst activity towards naphthalene decomposition was probably prevented by sulfur poisoning. Differences between the results of catalytic filters and non-catalytic filters stayed inside the limits of accuracy, which was estimated to be 5 %.

Without a catalyst, 48 % of toluene was decomposed at 900 ˚C. Most of the toluene decomposed to produce benzene and methane. With a nickel catalyst, 54 % of toluene was decomposed. Toluene, naphthalene and ethylene were decomposed and mainly methane, benzene and ethylene were formed. The main results calculated based on the experiments at 3 bar are shown in the Figure 15.

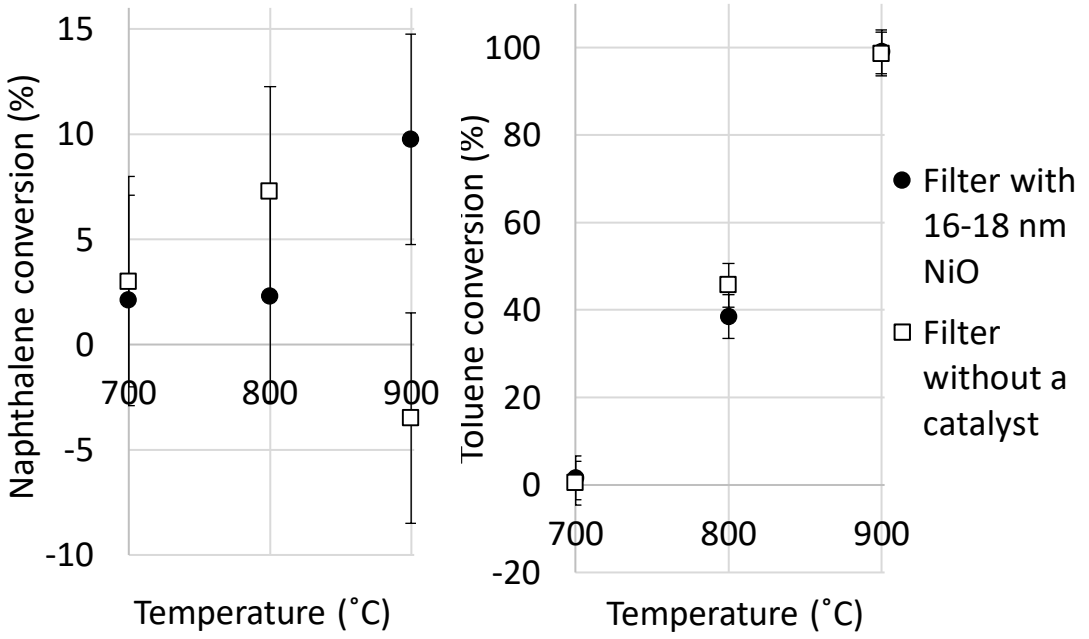

Figure 15. Conversions of naphthalene and toluene at 3 bar as a function of temperature with 1.5 l/min gas feed.

As shown in the Figure 15, also at 3 bar naphthalene conversions were low. Without a catalyst, conversions stayed below 7 % at each temperature. With a nickel catalyst, the conversion of 10 % was achieved at 900 °C. Due to sulfur in the gas, conversions at 700 and 800 °C were only around 2 % with a catalyst.

For toluene, conversions were almost doubled when the pressure was increased from 1 bar to 3 bar. Conversions of 98-99 % were achieved at 3 bar. Toluene, ethylene and

naphthalene seemed to decompose to form benzene and methane. Benzene was produced more at higher temperatures in all experiments. In addition, ethylene was decomposed more at higher temperatures mainly to produce methane. Some amounts of carbon were also produced during each experiment and later in the thesis, these amounts are analyzed in more detail. At lower pressures, there was less carbon formation on the surfaces. In literature, good filter performance with catalytic tar decomposition has been achieved even at atmospheric conditions with for example with the specific MgO supported nickel catalysts (Nacken , et al., 2015). This is probably due to the optimal process conditions, efficient catalyst and support system and lower surface velocities.

When compared to the lower pressures, at 5 bar more reasonable conversions for naphthalene decomposition reactions were achieved. Some of the main results at these conditions are shown in the Figure 16 as a function of temperature.

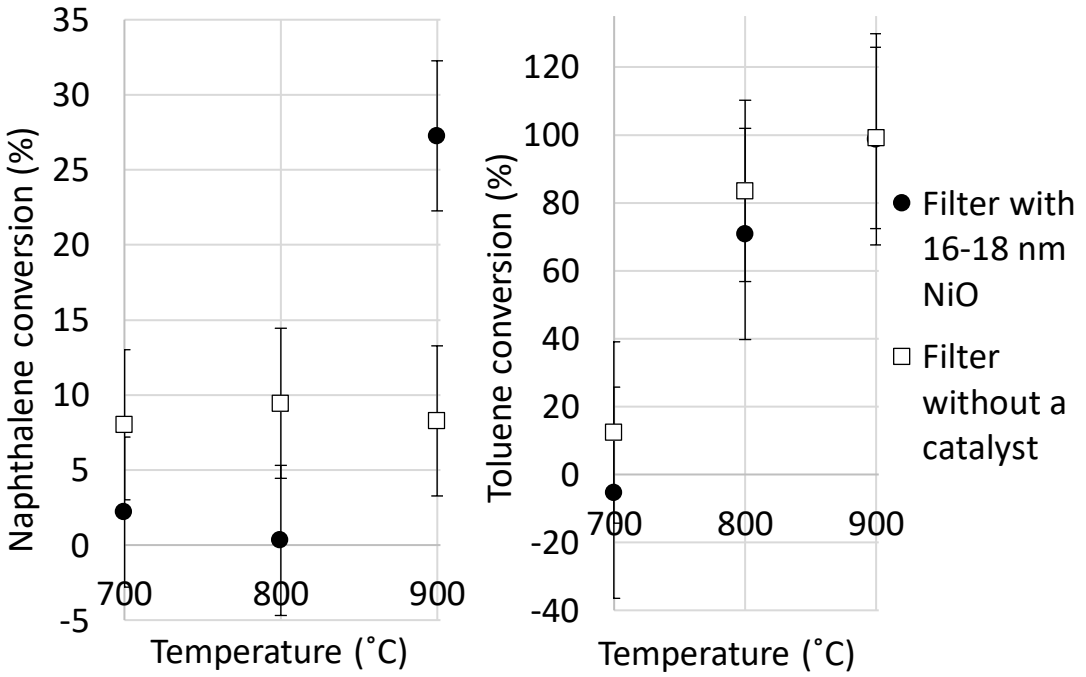

Figure 16. Conversions of naphthalene and toluene at 5 bar as a function of temperature with 1.5 l/min gas feed.

As can be seen from the Figure 16, naphthalene conversions were between 7-10 % in the experiments in which there was no catalyst applied. At lower pressures, these conversions stayed below 7 %. When the nickel coated catalyst was used at these conditions still no conversion of naphthalene occurred at temperatures between 700-800 ˚C but at 900 ˚C, conversion of 28 % was achieved. This was probably due to the high temperature, which increases the decomposition reaction rates of naphthalene but mainly due to the catalyst poisoning caused by the sulfur in the gas at lower temperatures. It has been reported that between temperatures of 800-900 ˚C there is sulfur desorption from the active Ni sites, which improves the naphthalene conversion. On the other hand, carbon deactivation is found to decrease when temperature is increased (Nacken , et al., 2015). Without a catalyst, conversion of naphthalene was affected less by the process temperature.

7.2 Effect of the gas face velocity

In addition to different pressures, also different surface velocities were tested. As mentioned in the chapter 6.2, the appropriate velocity could not be applied with the used process system and thus the effect of gas velocity on the naphthalene conversion needed to be estimated. From the literature and based on the equations shown in the earlier chapter, it could be assumed that by decreasing the face velocity the conversions of naphthalene would be improved (Zhao, et al., 2000).

In the Figure 17, the conversions of naphthalene and toluene are shown as a function of temperature with different gas feeding velocities. As mentioned in the chapter 4.1.2, gas face velocity is affected by the area of filtration surface and by the volumetric gas flow. Thus, the velocity increases when temperature is increased. The Figure 18 shows the conversions of naphthalene as a function of gas face velocity at 900 ˚C.

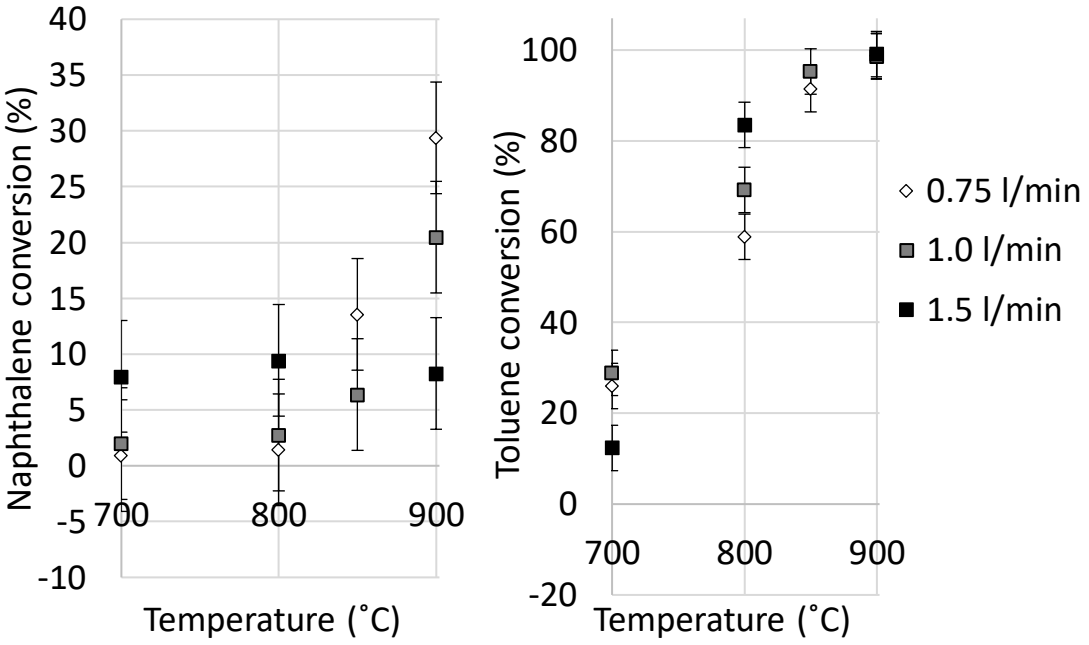

Figure 17. Conversions of naphthalene and toluene with a filter without a catalyst at 5 bar as a function of temperature.

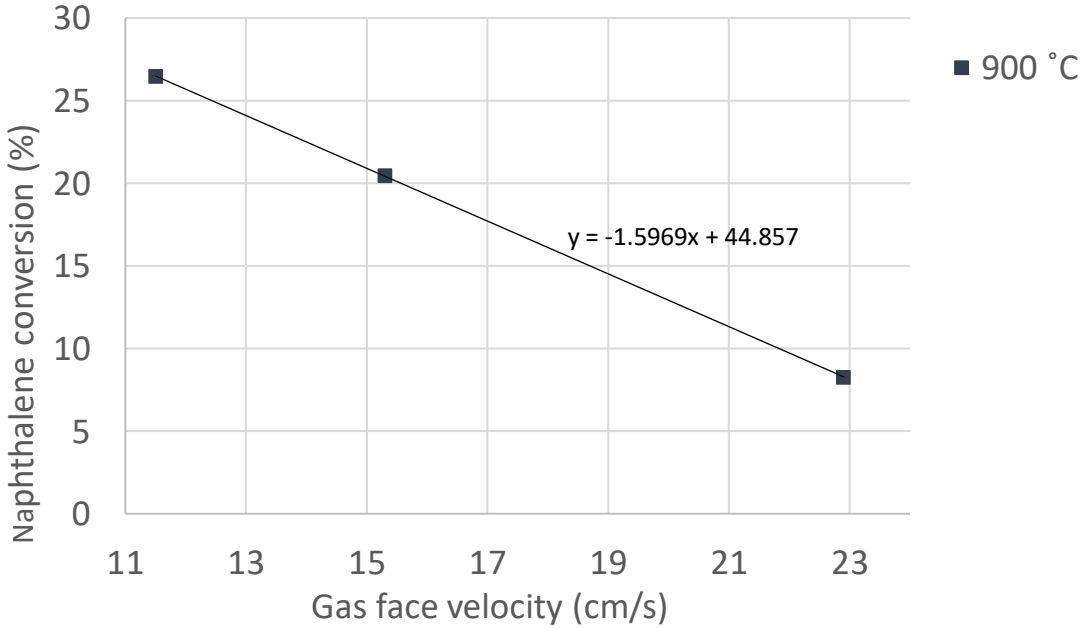

Figure 18. Conversion of naphthalene with a filter without a catalyst at 5 bar and at 900 ˚C as a function of face velocity.

From the Figure 17, it can be seen that the naphthalene conversion was not dependent on temperature with the highest gas velocity, but with lower velocities, the

naphthalene conversion increased with temperature. At 900 ˚C, the naphthalene conversion seemed to be almost linearly dependent on the temperature. Effect of face velocity on toluene conversion was opposite so that maybe some of the naphthalene was decomposed to form toluene instead of benzene at higher temperatures. More benzene was produced with lower surface velocities. With lower velocities, there was more time for tar decomposition reactions to take place on the filter surface, which might explain these results. If linear correlation for naphthalene conversion and face velocity was assumed, based on the Figure 18 it could be estimated that the conversion of 37 % could be achieved with 2.5 cm/s face velocity at 900 ˚C. The value of velocity had also strong effect on the pressure drop across the filter. Larger face velocities produced higher pressure drop across the filter. This result is supported by the information discussed in the chapter 4.1.2 and by the equation (27).

For nickel catalyst coatings, two different gas feed velocities of 1.0 and 1.5 l/min were tested. Naphthalene and toluene conversions as a function of reactor set point temperature are shown in the Figure 19.

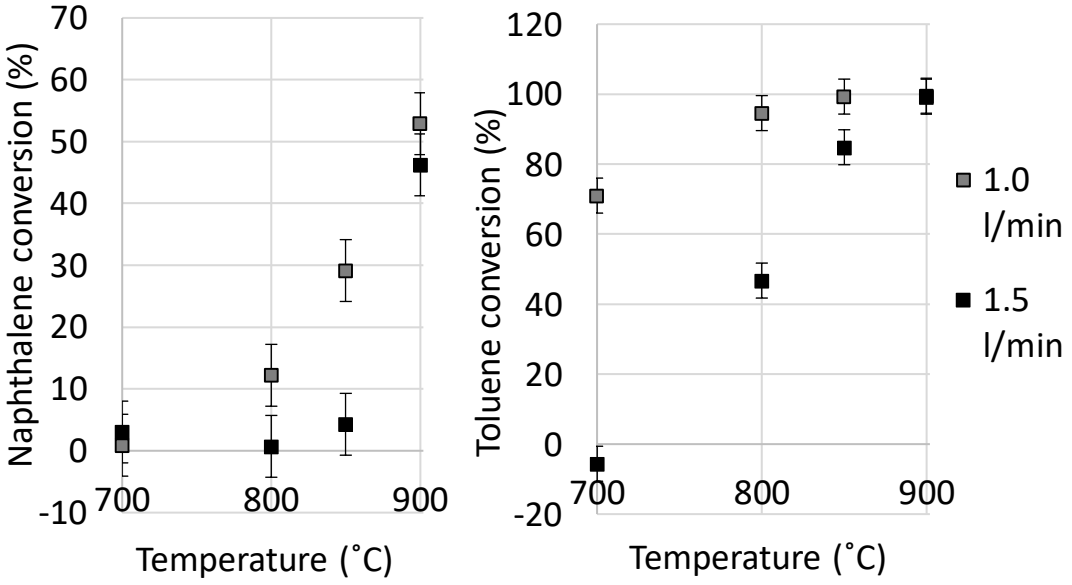

Figure 19. Conversions of naphthalene and toluene with 35-39 nm NiO and 11-12 nm Al_2O_3 at 5 bar as a function of temperature.

Same kind of behavior was seen with catalyst systems as was found with the filters without any catalyst when the surface velocities were studied. By lowering the gas face velocity of the fluid from 1.5 to 1.0 l/min, the conversion of naphthalene was increased from 46 % to 53 % at 900 ˚C. Toluene conversion was increased from 49 to 94 % at 800 ˚C and from 85 to 99 % at 850 ˚C. At 900 ˚C, toluene conversion stayed almost constant at values around 99 %. Additionally, less benzene and more methane were produced with lower surface velocities. If linear correlation would be assumed, naphthalene conversions of 68 % could be achieved at 900 ˚C with surface velocities of 2.5. cm/s.

7.3 Effect of the catalyst modifications

Experiments were done with metallic filters modified by ALD coatings. Nickel performed as a catalyst and Al_2O_3 as a support material. As a support, oxide compound can form large surface area on which a catalyst can stabilize as nanoparticles. This has been used to enhance catalyst dispersion on the medium (Romar, 2015; Zhang, et al., 2003). Additionally, the support has shown effect on the conversions due to the possible increase in number of active sites (Zhang, et al., 2003). It has been reported that alumina supports has caused increase in the carbon formation in some experiments (Trimm, 1985). Some experiments were done to study the effect of nickel catalyst amount on the naphthalene conversions. Conversions of naphthalene with different ALD coatings at 5 bar are shown as a function of temperature in the Figure 20 with gas feed of 1.5 l/min and in the Figure 21 with gas feed of 1.0 l/min.

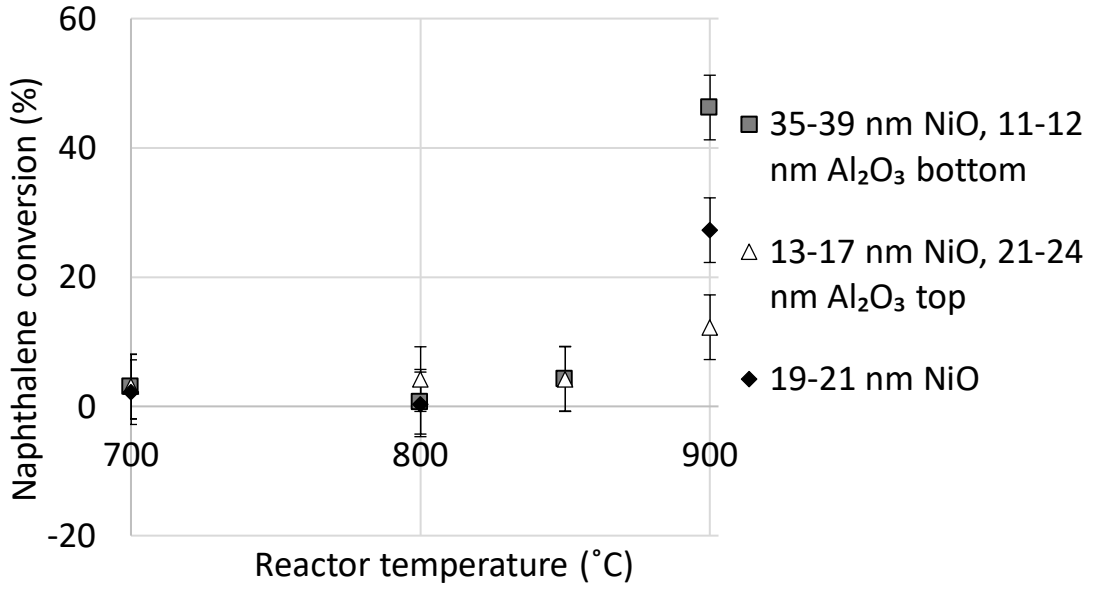

Figure 20. Conversion of naphthalene with different ALD coatings at 5 bar and with 1.5 l/min gas feed as a function of temperature.

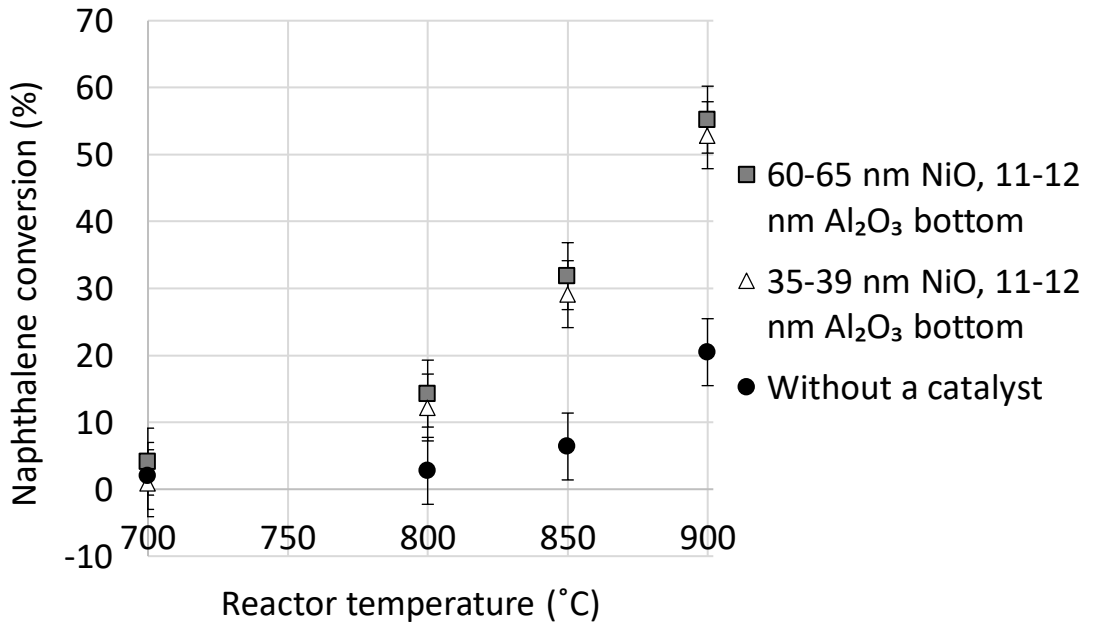

Figure 21. Conversion of naphthalene with different ALD coatings at 5 bar and with 1.0 l/min gas feed as a function of temperature.

The highest conversions were achieved with 60-65 nm NiO and 11-12 nm Al_2O_3. There was only small difference between 35-39 nm NiO and 60-65 nm NiO catalysts. 19-21 nm NiO catalyst performed only naphthalene conversions below 30 % probably both

due to the lack of the Al_2O_3 support and due to the lower amount of nickel catalyst. Alumina support had only slight effect on the naphthalene conversions. Amount of the support material was chosen based on the earlier experiments performed at VTT. Toluene conversion was not changed when more NiO was used but smaller amounts of benzene was produced.

7.4 Catalyst resistance towards sulfur and towards accumulated carbon

One experiment was done without hydrogen sulfide in the gas to study its effect on the nickel catalyst behavior. The main results are shown with the Figure 22.

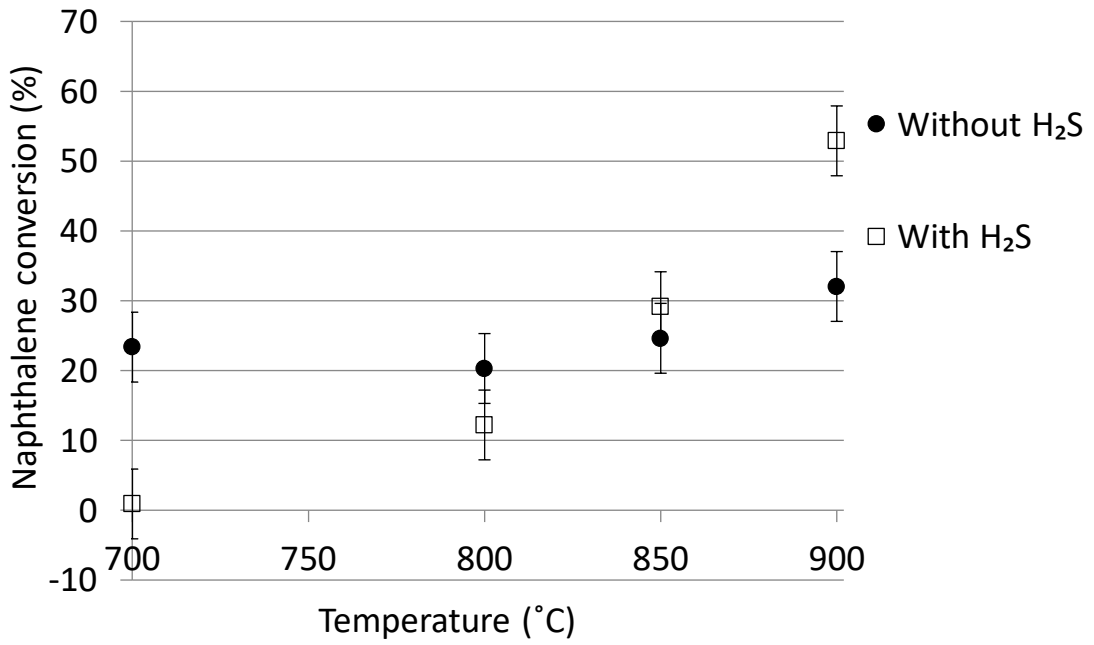

Figure 22. Conversion of naphthalene with and without hydrogen sulfide present in the gas at 5 bar and with 1.0 l/min gas feed as a function of temperature.

From the Figure 22, it can be seen that the sulfur had an effect on the naphthalene decomposition at temperatures below 850 ˚C and it prevented the naphthalene decomposition entirely at 700 ˚C. Sulfur did not have a significant effect on the toluene conversion but benzene was produced more when there was no sulfur present because more naphthalene was decomposed. Sulfur blocked the active sites of nickel catalyst at temperatures around 700 ˚C. At higher temperatures, there occurs

hydrogen sulfide desorption so that active nickel sites are free for decomposition reactions (Nacken , et al., 2015).

Pressure drop as a function of time at different temperature ranges is shown in the Figure 23 for filter system with 35-39 nm NiO and 11-12 nm Al_2O_3. All the experiments in which the catalyst was used showed quite similar behavior related to the pressure drop and all the average pressure drops can be found in the Appendix 4.

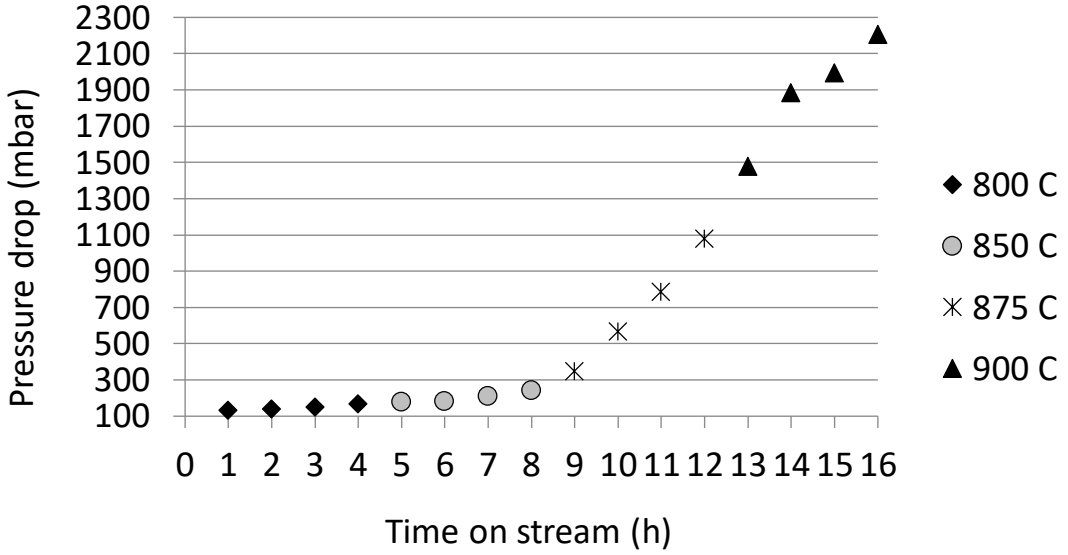

Figure 23. The pressure drop across the filter medium as a function of time on stream at 5 bar with 35-39 nm NiO and 11-12 nm Al_2O_3.

In each experiment in which nickel catalyst was applied at 5 bar, the pressure drop started to increase strongly at 850 ˚C. Without a catalyst coating, the pressure difference across the filter was almost constant through the experiments with increase staying below 220 mbar. By increasing the gas face velocity, the pressure drop increased as well. This was probably one of the reasons why in the literature pressure drops seem to be around 40-45 mbar with 2.5 cm/s gas face velocities (Simeone, et al., 2010). Increase in pressure drop was most probably caused by the carbon formation. Pictures of reactors without and with a catalyst after the experiments are shown in the Figure 24. In spite of carbonization and high increase in the pressure drop, conversions of naphthalene remained constant at high temperature. This means that the catalyst active sites were not blocked by carbon and decomposition of tar

components was not prevented. High temperatures have also been reported to increase the reaction rate of steam gasification of deposited carbon and thus decrease the deactivation caused by accumulated carbon (Nacken , et al., 2015).

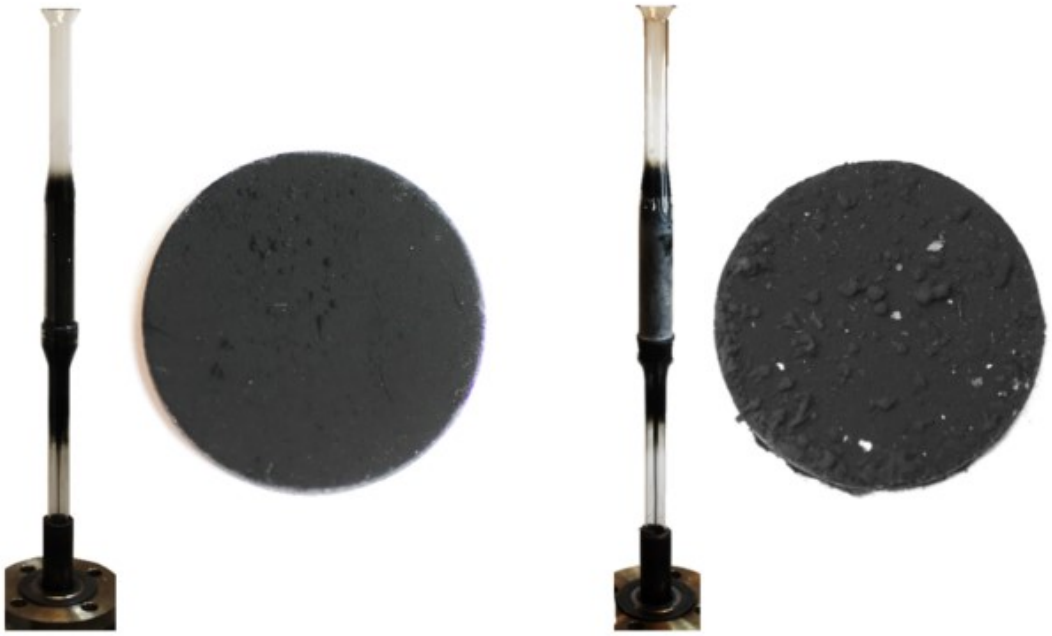

Figure 24. Filter without a catalyst on the left side and filter with 40-45 nm NiO and 11-12 nm alumina support on the right side after the experiments at 5 bar.

Even though with the experiments without a catalyst there was no significant pressure increase during the tests when compared to the catalytic systems, the surfaces of reactor and filter medium were covered with a thin carbon layer. Carbon on the catalytic filter medium was thicker, harder and more fragile when compared to the carbon formed on the non-catalytic filter medium. With a catalyst, there were probably more tar components on the filter medium, which affected the structure of the filter cake.

The results of increased weights of filter mediums can be found in the Appendix 3. Without a catalyst, the weight of the formed cake on the filter increased from 84 to 154 mg when pressure was increased from 1 bar to 5 bar. When the time on stream at temperatures above 800 ˚C was increased, more filter cake was formed. On the other hand, when the gas feeding velocity was decreased for example from 1.0 to 0.75

l/min the weight of the formed cake was increased from 123 to 154 mg. Without a catalyst, the increase in the weights of filter cakes varied from 21 to 154 mg depending on the process conditions and gas face velocity.

With nickel catalyst, the weights of the formed cakes were between 200-386 mg. When the pressure was increased from 1 bar to 5 bar, the weight of the cake was increased only from 200 to 210 mg. Temperature, time on stream, amount of catalyst and gas feeding velocities seemed to have the strongest effects. For example, when the gas feeding velocity was decreased from 1.5 to 1.0 l/min, the weight of the produced cake increased from 299 to 357 mg. Additionally, when the amount of nickel was increased from 35-39 nm to 60-65 nm, the weight of filter cake was decreased from 325 mg to 299 mg with 1.5 l/min gas feed.

With some experiments, the gas analyzer results from the oxidation of the reactor and filter medium were utilized to evaluate the amount of carbon on the surfaces of the reactor and filter. The amount of formed carbon on the reactor walls was found to be around 200 mg. One filter without a catalyst was oxidized to see, that about 100 mg of carbon was formed on the filter surface and 57 mg of the increase in the filter medium weight was caused by some other components. Based on these experiments, it was noticed that the amount of formed carbon did not have a significant effect on the conversions and molar balances. Additional experiments and product analysis are required to achieve information about the components collected on the filter medium.

7.5 Distribution of tar compounds

Distribution of benzene, toluene and naphthalene in the product gas when no catalyst was used and with a nickel catalyst are shown in the Figures 25 and 26.

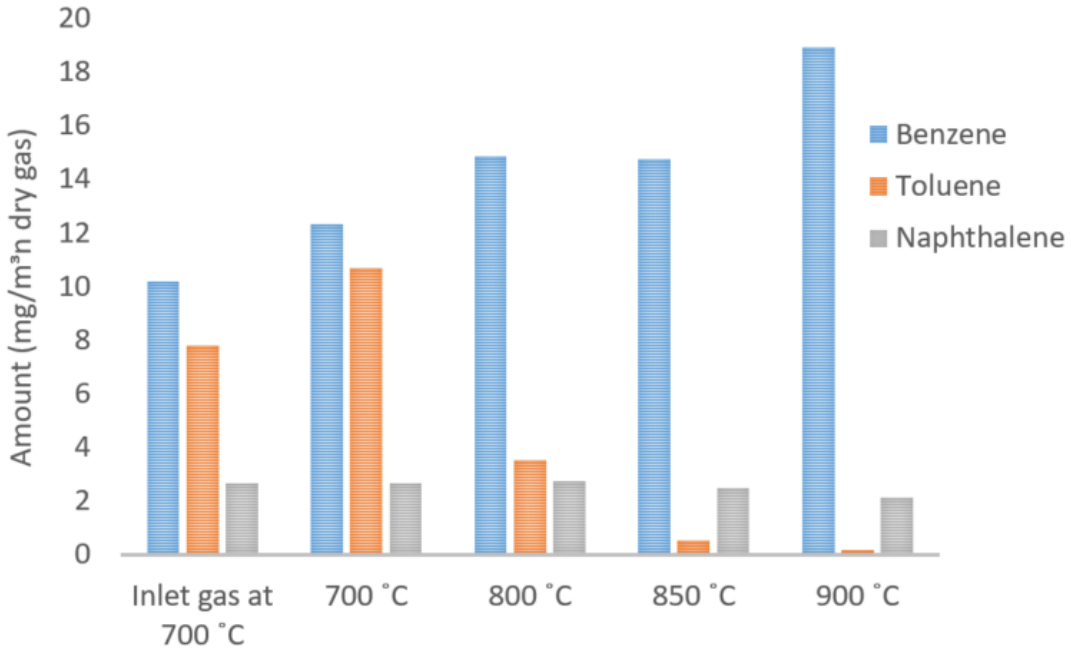

Figure 25. Amounts of tar components before and after the filter without a catalyst at 5 bar.

In the experiments, in which no catalyst was used, the amount of benzene was increased during the experiment but both naphthalene and toluene amounts were decreased. This suggests that naphthalene and toluene decomposed to form benzene in addition to other compounds. As already mentioned earlier, the amount of naphthalene started to decrease at temperatures above 850 ˚C.

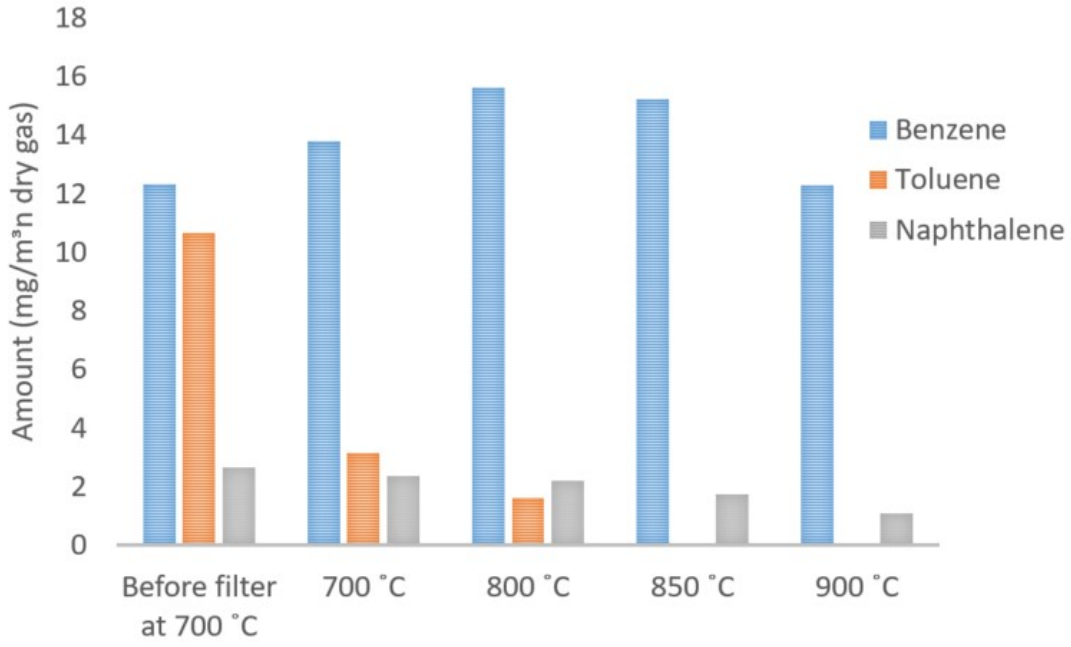

Figure 26. Amounts of tar components before and after the filter with 60-65 nm NiO and 11-12 nm Al_2O_3 catalyst at 5 bar.

In the experiments with nickel catalysts, amount of benzene increased only below 850 ˚C after which its amount started to decrease. At 900 ˚C, the amount of benzene decreased to the lower level that it was in the beginning. At these conditions benzene seemed to decompose as well to form methane. Toluene decomposed almost entirely at 850 ˚C and the amount of naphthalene decreased with increasing temperature. In some experiments described in the literature, naphthalene decomposition has formed toluene instead of benzene (Simeone, et al., 2010).

7.6 Error estimation

Conversions and amounts of tar compounds in the gas were calculated based on the data obtained from the online gas analyzer and from the gas chromatograph. The temperatures of the process lines and reactor were measured and controlled. There are possibility for errors due to imprecise calibrations, equipment properties and human actions. In the Table 7, the estimated errors for pressure controller of the reactor are listed, which are calculated based on the results from each different pressure set points.

Table 7. Set point pressures and errors calculated based on the experimental results of different pressure set points.

Run	Reactor T (˚C)	Set point pressure (bar)	Max error in pressure to set point pressure (%)
6	700-900	1.0	18.1
7	700-900	3.0	8.6
8	700-900	5.0	4.4
10	700-900	1.0	26.8
11	700-900	3.0	6.6
12	700-900	5.0	5.9
13	700-900	5.0	4.4
14	700-900	5.0	4.0
15	700-900	5.0	5.6
16	800-900	3.0	3.0
17	700-900	5.0	6.6
18	800-900	5.0	5.0
19	800-900	5.0	3.8
20	800-900	5.0	6.2
21	800-900	5.0	5.8
22	800- 900	3.0	5.9
24	800-900	5.0	3.4
25	800-900	5.0	3.5

Error due to the pressure controller was significant and needed to be noticed when estimating the reliability of the results. During the last hour of experiments at 900 ˚C, the pressure drop started to increase so much that the pressure controller could not control the pressure anymore. This was taken into account when calculating the results and this pressure increase was not included in the maximum pressure errors shown in the Table 7. After the first experiments, different pressure controller was used to achieve more accurate pressure control for the system.

The error in temperature control seemed to be around ±3 %. Temperature inside the reactor was affected by the endothermic or exothermic natures of the occurring reactions. Some error might be caused by the very small leakage in the bottom of the reactor that was noticed in the pressure tests and could not be removed entirely. The effects of the errors from the pressure and temperature variations on the results were minimized by choosing carefully the average stabilized values from the gas analyzer and gas chromatograph for calculations.

All the mass flow meters were calibrated before the experiments were started. The gas chromatograph was calibrated in the beginning of each experiments to minimize the errors. The limit of inaccuracy for gas analysis is estimated to be ±5 %. Three different total gas flows were applied during the experiments with some error level. The online gas analyzer was calibrated with pure nitrogen and with calibration gas mixture once in two weeks. Additionally, there are always some error caused by the human action during the laboratory tasks and due to the calculation methods. There was also possibility for condensation of tar components in the process lines, but this was minimized by the proper insulating and heating of the lines. The process lines were cleaned carefully with purge nitrogen before and after each experiments.

8 Conclusions and proposals for future studies

When considering the aim of studying the catalytic activity and performance of novel filter materials for tars decomposition, the thesis carried out several successful experiments for the decomposition reactions. These results were compared with the results achieved from the experiments with nickel-coated filters. Catalysts were applied on the filter medium by ALD method and several different catalyst configurations were tested as well as different process conditions were studied. Some catalytic activity was achieved with metal filters without any catalysts at 5 bar. Naphthalene conversions did not increase above 25 % in any applied conditions without a catalyst. With ALD nickel coatings, 65 % naphthalene conversions were reached at 900 ˚C with stable catalyst but problems related to the carbonization of the reactor occurred. At temperatures above 850 ˚C with nickel catalyst, pressure drop increased quickly and finally the reactor was blocked. Without a catalyst, filters did not have problems related to the reactor clogging even though visible carbon film was formed on the walls and on the surface of the filter medium.

Suitable nickel-catalyst systems are fascinating to study due to their low price when compared for example with noble catalyst options. They have high potential in tar decomposition applications due to their high activity towards these reactions and their high stability in the process conditions. It would be important to find out how to meet both the challenges related to reactor coking and to sulfur poisoning. Additionally, catalytic activity towards the challenging tar components such as naphthalene should be as high as possible. Other supports and promoters such as MgO are recommended to study to achieve better performance for nickel catalyst. Filtration unit has potential to work as a pre-reformed unit but still there is need for the actual reformer reactor to achieve the required purity for the FT-synthesis. Pre-reformer could prevent carbon accumulation in the reformer reactor caused by the heavy tar components. Due to the ALD method, only small amount of catalyst is needed to achieve high conversions of tar components and thus it might be useful to study the noble metal catalysts applied

with this method in more detail as well. Suitable noble metal catalyst would be for example rhodium based on the earlier studies.

Few important limitations concerning this experimental setup were the lack of actual ash on the filter medium and too large surface velocities, which reduced the reliability and comparability of the results. Cleaning of the filter medium by back pulse technique could not been studied with the system to see if the sticky cake could have been flushed with the gas. In the future research, there would be interest to study the catalytic activity of gasifier bed materials and ash formed in gasifier towards tar decomposition on the filter medium.

Bibliography

Abdoulmoumine, N., Adhikari, S., Kulkarni, A. & Chattanathan, S., 2015. A review on biomass gasification syngas cleanup. *Appl. Energ.,* Volume 155, pp. 294-307.

Agilent Technologies, Inc., 2010. *Agilent 7890A Gas Chromatograph Operating Guide,* Wilmington, USA.

Allesina, G. et al., 2014. Porous filtering media comparison through wet and dry sampling of fixed bed gasification. *J. Phys.: Conference Series,* Issue 547, pp. 1-9.

Alonso-Fariñas, B., Lupion, M., Rodriguez-Galan, M. & Martinez-Fernandez, J., 2013. New candle prototype for hot gas filtration industrial applications. *Fuel,* Volume 114, pp. 120-127.

André, R. N. et al., 2005. Fluidised bed co-gasification of coal and olive oil industry wastes. *Fuel,* Volume 84, pp. 1635–1644.

Asadullah, M., 2014. Biomass gasification gas cleaning for downstream applications: A comparative critical review. *Renew. Sust. Energ. Rev.,* Volume 40, pp. 118-132.

Asadullah, M. et al., 2002. Biomass Gasification to Hydrogen and Syngas at Low Temperature: Novel Catalytic System Using Fluidized-Bed Reactor. *J. Catal.,* Volume 208, pp. 255-259.

Aznar, M. P. et al., 1998. Commercial Steam Reforming Catalysts To Improve Biomass Gasification with Steam−Oxygen Mixtures. 2. Catalytic Tar Removal. *Ind. Eng. Chem.,* 37(7), pp. 2668-2680.

Babu, S., 1995. Thermal gasification of biomass technology developments: End of task report. *Biomass Bioenerg.,* 9(1-5), pp. 271-285.

Baker, E. G. & Mudge, L. K., 1984. *Catalysis in Biomass Gasification.* U.S. Pacific Northwest Laboratory: Battelle.

Baker, E. G., Mudge, L. K. & Brown, M. D., 1987. Steam Gasification of Biomass with Nickel Secondary Catalysts. *Ind. Eng. Chem. Res.,* Volume 26, pp. 1335-1339.

Balonek, C. M. et al., 2010. Effect of Alkali Metal Impurities on Co–Re Catalysts for Fischer–Tropsch Synthesis from Biomass-Derived Syngas. *Catal. Lett.,* Volume 138, pp. 8-13.

Basu, P., 2013. *Biomass Gasification, Pyrolysis and Torrefaction: Practical Design and Theory.* Lontoo: Elsevier Inc..

Bergiorno, V., Feo, G. D., Della Rocca, C. & Napoli, R. M. A., 2003. Energy from gasification of solid wastes. *Waste Manage.,* Volume 23, pp. 1-15.

Boerrigter, H., den Uil, H. & Calis, H.-P., 2002. *Green Diesel from Biomass via Fischer-Tropsch synthesis: New Insights in Gas Cleaning and Process Design.* Strasbourg, France, Pyrolysis and Gasification of Biomass and Waste, Expert Meeting.

Cavattoni, T. & Garbarino, G., 2017. Catalytic abatement of biomass tar: a technological perspective of Ni-based catalysts. *Rend. Fis. Acc. Lincei,* 28(1), pp. 69-85.

Cheng, Y.-H. & Tsai, C.-J., 1998. Factors Influencing Pressure Drop through a Dust Cake during Filtration. *Aerosol Sci. Technol.,* 29(4), pp. 315-328.

Chung, J.-D., Hwang, T.-W. & Park, S.-J., 2003. Filtration and Dust Cake Experiment by Ceramic Candle Filter in High Temperature Conditions. *Korean J. Chem. Eng,* 20(6), pp. 1118-1122.

Constantinou, D. A., Fierro, J. L. G. & Efstathiou, A. M., 2010. Acomparative study of the steam reforming of phenol towards H2 production over natural calcite, dolomite and olivine materials. *Appl. Catal. B-Environ.,* Volume 95, pp. 255-269.

Cummer, K. R. & Brown, R. C., 2002. Achillary equipment for biomass gasification. *Biomass Bioenerg.,* Volume 23, pp. 113-128.

Dayton, D. C., French, R. J. & Milne, T. A., 1995. Direct Observation of Alkali Vapor Release during Biomass Combustion and Gasification. 1. Application of Molecular Beam/Mass Spectrometry to Switchgrass Combustion. *Energ. Fuel.,* Volume 9, pp. 855-865.

de Jong, W. et al., 2003. Biomass and fossil fuel conversion by pressurised fluidised bed gasification using hot gas ceramic filters as gas cleaning. *Biomass Bioenerg.,* Volume 25, pp. 59-83.

de Souza-Santos, M. L., 2004. *Solid fuels combustion and gasification : modeling, simulation, and equipment operation.* 1 ed. New York: Marcel Dekker cop..

Devi, L. et al., 2005. Catalytic decomposition of biomass tars: use of dolomite and untreated olivine. *Renew. Energ.,* Volume 30, pp. 565-587.

D'Orazio, A. et al., 2015. Gas conditioning in H2 rich syngas production by biomass steam gasification: Experimental comparison between three innovative ceramic filter candles. *Int. J. Hydrogen Energ.,* Volume 40, pp. 7282-7290.

Dou, B. et al., 2007. Single and Combined Removal of HCl and Alkali Metal Vapor from High-temperature Gas by Solid Sorbents. *Energy & Fuels,* Volume 21, pp. 1019-1023.

Dou, B. et al., 2002. High-Temperature Removal of NH3, Organic Sulfur, HCl, and Tar Component from Coal-Derived Gas. *Ind. Eng. Chem. Res.,* Volume 41, pp. 4195-4200.

Enerdata, Global Energy Statistical Yearbook, 2017. *Global Energy Statistical Yearbook 2017.* [Online] Available at: https://yearbook.enerdata.net/ [Accessed 10 November 2017].

Engelen, K., Zhang, Y., Draelants, D. J. & Baron , G. V., 2003. A novel catalytic filter for tar removal from biomass gasification gas: Improvement of the catalytic activity in presence of H2S. *Chem. Eng. Sci.,* Volume 58, pp. 665-670.

Farzad, S., Mandegari, M. A. & Görgens, J. F., 2016. A critical review on biomass gasification, co-gasification, and their environmental assessment. *Biofuel Res. J.,* Volume 12, pp. 483-495.

Furusawa, T. & Tsutsumi, A., 2005. Comparison of Co/MgO and Ni/MgO catalysts for the steam reforming of naphthalene as a model compound of tar derived from biomass gasification. *Appl. Catal. A-Gen.,* Volume 278, pp. 207-212.

Fushimi, C., Araki, K., Yamaguchi, Y. & Tsutsumi, A., 2003. Effect of Heating Rate on Steam Gasification of Biomass. 2. Thermogravimetric-Mass Spectrometric (TG-MS) Analysis of Gas Evolution. *Ind. Eng. Chem. Res.,* Volume 42, pp. 3929-3936.

Gao, N., Li, A., Quan, C. & Gao, F., 2008. Hydrogen-rich gas production from biomass steam gasification in an updraft fixed-bed gasifier combined with a porous ceramic reformer. *Int. J. Hydrogen Energ.,* Volume 33, pp. 5430-5438.

Garcia, L., French, R., Czernik, S. & Chornet, E., 2000. Catalytic steam reforming of bio-oils for the production of hydrogen: effects of catalyst composition. *Appl. Catal. A-Gen.,* 201(2), pp. 225-239.

Ghidossi, R. et al., 2009. Separation of particles from hot gases using metallic foams. *J. Mater. Process. Technol.,* Volume 209, pp. 3859-3868.

Gil, J., Corella, J., Aznar, M. P. & Caballero, M. A., 1999. Biomass gasification in atmospheric and bubbling fluidized bed: Effect of the type of gasifying agent on the product distribution. *Biomass Bioenerg.,* Volume 17, pp. 389-403.

González-Carballo, J. & Fierro, J., 2010. Fundamentals of syngas production and Fischer-Tropsch synthesis. In: *Biofuels from Fischer-Tropsch synthesis.* New York: Nova Science Publishers, Inc., pp. 1-33.

Good, J. et al., n.d. *Sampling and analysis of tar and particles in biomass producer gases - Technical Report*.

Guan, G., Kaewpanha, M., Hao, X. & Abudula, A., 2016. Catalytic steam reforming of biomass tar: Prospects and challenges. *Renew. Sust. Energ. Rev.,* Volume 58, pp. 450–461.

Guan, X., Gardner, B., Martin, R. A. & Spain, J., 2008. Demonstration of hot gas filtration in advanced coal gasification system. *Powder Technol.,* 180(1-2), pp. 122-128.

Gupta, R., Turk, B. S., Portzer, J. W. & Cicero, D. C., 2001. Desulfurization of Syngas in a Transport Reactor. *Environ. Prog.,* 20(3), pp. 187-195.

Gustafsson, E., Strand, M. & Sanati, M., 2007. Physical and Chemical Characterization of Aerosol Particles Formed during the Thermochemical Conversion of Wood Pellets Using a Bubbling Fluidized Bed Gasifier. *Energ. Fuel.,* Volume 21, pp. 3660-3667.

Göransson, K., Söderlind, U., He, J. & Zhang, W., 2011. Review of syngas production via biomass DFBGs. *Renew. Sust. Energ. Rev.,* Volume 15, pp. 482-492.

Hamelinck, C. N., Faaij , A. ´. P., den Uil , H. & Boerrigter, H., 2004. Production of FT transportation fuels from biomass; technical options, process analysis and optimisation, and development potential. *Energy,* Volume 29, pp. 1743–1771.

Hannula, I. & Kurkela , E., 2013. Liquid transportation fuels via large-scale fluidised-bed gasification of lignocellulosic biomass. *VTT Technol.,* Volume 91, pp. 1-126.

Hasler, P. & Nussbaumer, T., 1999. Gas cleaning for IC engine applications from fixed bed biomass gasification. *Biomass Bioenerg.,* Volume 16, pp. 385-395.

Heidenreich, S., 2013. Hot gas filtration – A review. *Fuel,* Volume 104, pp. 83-94.

Heidenreich, S. et al., 2002. Hot gas filtration with ceramic filters: Experiences and new developments. *Filtr. Separat.,* 39(4), pp. 22-25.

Hemmer, G., Hoff, D. & Kasper, G., 2003. Thermo-analysis of fly ash and other particulate materials for predicting stable filtration of hot gases. *Adv. Powder Technol.,* Volume 14, pp. 631-655.

Hepola, J. & Simell, P., 1997. Sulphur poisoning of nickel-based hot gas cleaning catalysts in synthetic gasification gas II. Chemisorpotion of hydrogen sulpide. *Appl. Catal. B-Environ.,* Volume 14, pp. 305-321.

Higman, C. & van der Burgt, M., 2003. *Gasification.* Oxford: Elsevier.

Hofmann, P. et al., 2008. Integrating biomass gasification with solid oxide fuel cells: Effect of real product gas tars, fluctuations and particulates on Ni-GDC anode. *Int. J. Hydrogen Energ.,* Volume 33, pp. 2834-2844.

Hognon, C., Dupont, C., Grateau, M. & Delrue, F., 2014. Comparison of steam gasification reactivity of algal and lignocellulosic biomass: Influence of inorganic elements. *Bioresource Technol.,* Volume 164, pp. 347-353.

http://www.vtt.fi/sites/BTL2030, September 2017. *BTL2030 2016-2018.* [Online] Available at: http://www.vtt.fi/sites/BTL2030 [Accessed 20 October 2017].

Hu, G. et al., 2006. Steam gasification of apricot stones with olivine and dolomite as downstream catalysts. *Fuel Process. Technol.,* 87(5), pp. 375-382.

Hurley, J. P., Mukherjee, B. & Mann, M. D., 2006. Assessment of Filter Dust Characteristics that Cause Filter Failure during Hot-Gas Filtration. *Energ. Fuel.,* Volume 20, pp. 1629-1638.

Höök, M. & Xu, T., 2013. Depletion of fossil fuels and anthropogenic climate change - a review. *Energ. Policy,* Volume 52, pp. 797-809.

Jazbec, M., Sendt, K. & Haynes , B. S., 2004. Kinetic and thermodynamic analysis of the fate of sulphur compounds in gasification products. *Fuel,* Volume 83, pp. 2133-2138.

Jha, D. S., Sekellick, R. S., Rubow, D. K. L. & Corporation Mott, 1999. *Sintered metal hot gas filters.* Karlsruhe, Germany, Presented at the 4th International Symposium Gas Cleaning at High Temperatures.

Johnson, R. W., Hultqvist, A. & Bent, S. F., 2014. A brief review of atomic layer deposition: from fundamentals to applications. *Mater. Today,* 17(5), pp. 236-26.

Juutilainen, S. J., Simell, P. A. & Krause, A. O. I., 2006. Zirconia: Selective oxidation catalyst for removal of tar and ammonia from biomass gasification gas. *Appl. Catal. B-Environ.,* Volume 62, pp. 86-92.

Kaisalo, N., 2017. *Tar reforming in biomass gasification gas cleaning,* Helsinki: School of Chemical Engineering.

Kaisalo, N., Kihlman, J., Hannula, I. & Simell, P., 2015. Reforming solutions for biomass-derived gasification gas – Experimental. *Fuel,* Volume 147, pp. 208–220.

Kim, J.-H., Kim, Y.-C. & Choi, J.-H., 2016. Characteristics of pressure drop during the pulse-jet cleaning of a ceramic filter for high temperature and high pressure. *Korean J. Chem. Eng.,* 33(2), pp. 726-734.

Kim, J.-H.et al., 2008. Temperature effect on the pressure drop across the cake of coal gasification ash formed on a ceramic filter. *Powder Technol.,* 181(1), pp. 67-73.

Knudsen, M. & Weber, R., 1911. Resistance to motion of small spheres. *Ann. Phys.,* Volume 36, pp. 981-984.

Kuchonthara, P., Vitidsant, T. & Tsutsumi, A., 2008. Catalytic effects of potassium on lignin steam gasification with γ-Al2O3 as a bed material. *Korean J. Chem. Eng.,* 25(4), pp. 656-662.

Kurkela, E., Kurkela , M. & Hiltunen, I., 2016. Steam–oxygen gasification of forest residues and bark followed by hot gas filtration and catalytic reforming of tars: Results of an extended time test. *Fuel Process. Technol.,* Volume 141, pp. 148-158.

Kurkela, E. & Ståhlberg, P., 1992. Air gasification of peat, wood and brown coal in a pressurized fluidized-bed reactor. I. Carbon conversion, gas yields and tar formation. *Fuel Process. Technol.,* Volume 31, pp. 1-21.

Leppälahti, J. & Koljonen, T., 1995. Nitrogen evolution from coal, peat and wood during gasification: Literature review. *Fuel Process. Technol.,* Volume 43, pp. 1-45.

Leppälahti, J., Simell, P. & Kurkela, E., 1991. Catalytic conversion of nitrogen compounds in gasification gas. *Fuel Process Technol.,* Volume 29, pp. 43-56.

Li, C. & Suzuki, K., 2009. Tar property, analysis, reforming mechanism and model for biomass gasification—An overview. *Renew. Sust. Energ. Rev.,* Volume 13, pp. 594–604.

Li, D., Tamura, M., Nakagawa, Y. & Tomishige, K., 2015. Metal catalysts for steam reforming of tar derived from the gasification of lignocellulosic biomass. *Bioresource Technol.,* Volume 178, pp. 53-64.

Li, S. et al., 2002. Promoted Iron-Based Catalysts for the Fischer-Tropsch Synthesis: Design, Synthesis, Site Densities and Catalytic Properties. *J. Catal.,* Volume 206, pp. 202-217.

Li, X. et al., 2004. Biomass gasification in a circulating fluidized bed. *Biomass Bioenerg.,* Volume 26, pp. 171–193.

Lupión, M., Ortiz, F. J. G., Navarrete, B. & Cortés , V. J., 2010. Assessment performance of high-temperature filtering elements. *Fuel,* Volume 89, pp. 848-854.

Lupion, M., Rodriguez-Galan, M., Alonso-Fariñas, B. & Gutierrez Ortiz, F., 2014. Investigation into the parameters of influence on dust cake porosity in hot gas filtration. *Powder Technol.,* Volume 264, pp. 592-598.

Maihak AG, Werner, J., 2000. *S700 Series, Extractive Gas Analyzers User Instructions,* Hamburg: Maihak AG.

Mai, R. et al., 2002. *Operation Behavior of a Multi-Candle Filter with Coupled Pressure Pulse Recleaning during Normal Operation and in the Case of a Filter Candle Failure.* Morgantown, United States, Conference: 5th International Symposium on Gas Cleaning at High Temperatures.

Maitlis, P. M., 2013. What is Fischer-Tropsch. In: P. M. Maitlis, ed. *Greener Fischer-Tropsch Processes for Fuels and Feedstocks* . 1 ed. Weinheim: John Wiley & Sons, Incorporated, pp. 3-19.

Ma, L., Verelst, H. & Baron, G. V., 2005. Integrated high temperature gas cleaning: Tar removal in biomass gasification with a catalytic filter. *Catal. Today,* 105(3-4), pp. 729-734.

Marichy, C., Bechelany, M. & Pinna, N., 2012. Atomic Layer Deposition of Nanostructured Materials for Energy and Environmental Applications. *Adv. Mater.,* pp. 1-16.

Mathieu, P. & Dubuisson, R., 2002. Performance analysis of a biomass gasifier. *Energ. Convers. Manage.,* Volume 43, pp. 1291–1299.

McKendry, P., 2002a. Energy production from biomass (part 2): conversion technologies. *Bioresource Technol.,* Volume 83, pp. 47–54 Review.

McKendry, P., 2002b. Energy production from biomass (part 3): gasification technologies. *Bioresource Technol.,* Volume 83, pp. 55–63.

Miikkulainen, V., Leskelä, M., Ritala, M. & Puurunen, R. L., 2013. Crystallinity of inorganic films grown by atomic layer deposition: Overview and general trends. *J. Appl. Phys.,* Volume 113, pp. 1-99.

Milne, T. & Evans, R., 1998. *Biomass Gasifier "Tars": Their Nature, Formation, and Conversion,* Golden, Colorado.

Mitsuoka, K. et al., 2011. Gasification of woody biomass char with CO2: The catalytic effects of K and Ca species on char gasification reactivity. *Fuel Process. Technol.,* 92(1), pp. 26-31.

Moersch, O., Spliethoff, H. & Hein, K., 2000. Tar quantification with a new online analyzing method. *Biomass Bioenerg.,* Volume 18, pp. 79-86.

Mohammed, I. Y., Samah, M., Mohamed, A. & Sabina, G., 2014. Comparison of SelexolTM and Rectisol® Technologies in an Integrated Gasification Combined Cycle (IGCC) Plant for Clean Energy Production. *Int. J. Eng. Res.,* 3(12), pp. 742-744.

Mondal, P., Dang, G. S. & Garg, M. O., 2011. Syngas production through gasification and cleanup for downstream applications — Recent developments. *Fuel Process. Technol.,* Volume 92, pp. 1395-1410.

Mudge, L. K., Baker, E. G., Brown, M. D. & Wilcox, W. A., 1987. *Bench-Scale Studies on Gasification of Biomass in the Presence of Catalysts.* U.S. Pacific Northwest Laboratory: Battelle.

Mukhopadhyay, A., Pandit, V. & Dhawan, K., 2016. Effect of high temperature on the performance of filter fabric. *J. Ind. Text.,* 45(6), pp. 1587-1602.

Nacken , M. et al., 2015. New DeTar catalytic filter with integrated catalytic ceramic foam: Catalytic activity under model and real bio syngas conditions. *Fuel Process. Technol.,* Volume 134, pp. 98–106.

Nacken, M., Ma, L., Heidenreich, S. & Baron, G. V., 2009. Performance of a catalytically activated ceramic hot gas filter for catalytic tar removal from biomass gasification gas. *Appl. Catal. B-Environ.,* Volume 88, pp. 292-298.

Nacken, M., Ma, L., Heidenreich, S. & Baron, G. V., 2010. Catalytic Activity in Naphthalene Reforming of Two Types of Catalytic Filters for Hot Gas Cleaning of Biomass-Derived Syngas. *Ind. Eng. Chem. Res.,* Volume 49, pp. 5536-5542.

Nacken, M. et al., 2012. Development of a catalytic ceramic foam for efficient tar reforming of a catalytic filter for hot gas cleaning of biomass-derived syngas. *Appl. Catal. B-Environ.,* Volume 125, pp. 111-119.

Narváez, I., Orío, A., Aznar, M. P. & Corella, J., 1996. Biomass Gasification with Air in an Atmospheric Bubbling Fluidized Bed. Effect of Six Operational Variables on the Quality of the Produced Raw Gas. *Ind. Eng. Chem. Res.,* Volume 35, pp. 2110-2120.

Ojeda, M. & Rojas, S., 2010. *Biofuels from Fischer-Tropsch Synthesis RUSH.* 1st ed. New York: Nova Science Publishers, Inc. .

O'Neill, B. J. et al., 2015. Catalyst Design with Atomic Layer Deposition. *ACS Catal.,* Volume 5, pp. 1804-1825.

Our World in Data, 2017. *Our World in Data.* [Online] Available at: https://ourworldindata.org/energy-production-and-changing-energy-sources [Accessed 10 November 2017].

Pallozzi, V. et al., 2016. Performance evaluation at different process parameters of an innovative prototype of biomass gasification system aimed to hydrogen production. *Energ. Convers. Manage.,* Volume 130, pp. 34–43.

Pinto, F. et al., 2010. Co-gasification of coal and wastes in a pilot-scale installation. 2: Effect of catalysts in syngas treatment to achieve sulphur and nitrogen compounds abatement. *Fuel,* Volume 89, pp. 3340-3351.

Pitcher , W. H. J., 1982. *Honeycomb filter and method of making it.* s.l. Patent No. US 4417908 A.

Pour, N., Housaindokht, M. R., Tayyari, S. F. & Zarkesh, J., 2010. Kinetics of the water-gas shift reaction in Fischer-Tropsch synthesis overa nano-structured iron catalyst. *J. Nat. Gas Chem.,* Volume 19, pp. 362-368.

Premium Engineering, 2016. *What is Gasification?.* [Online] Available at: http://www.premen.ru/en/content/gasification/ [Accessed 25 October 2017].

Punjak, W. A., Uberoi, M. & Shadman, F., 1989. *Control of ash deposition through the high temperature adsorption of alkali vapors on solid sorbents.* s.l., Proceedings of the ACS national meeting.

Puurunen, R., 2005. Surface chemistry of atomic layer deposition: a case study for the trimethylaluminum/water process. *J. Appl. Phys.,* 97(12), pp. 1-52.

Rajvanshi, A. K., 1986. Biomass gasification. In: D. Y. Goswami, ed. *Alternative Energy in Agriculture.* Maharashtra: CRC Press, pp. 83-102.

Rapagnà , S. et al., 2009. In Situ Catalytic Ceramic Candle Filtration for Tar Reforming and Particulate Abatement in a Fluidized-Bed Biomass Gasifier. *Energ. Fuel.,* Volume 23, pp. 3804-3809.

Ripperger, S., Gösele, W. & Alt, C. eds., 2012. Filtration, 1. Fundamentals. In: *Ullmann's Encyclopedia of Industrial Chemistry.* Weinheim: Wiley-VCH Verlag GmbH & Co. KGaA, pp. 678-708.

Rodionova, M. V. et al., 2016. Biofuel production: Challenges and opportunities. *Int. J. Hydrogen Energ.,* pp. 1-12.

Romar, H., 2015. *Biomass gasification and catalytic conversion of synthesis gas.* Tampere: Juvenes print.

Rotrupnielsen, J., 1971. Some principles relating to the regeneration of sulfur-poisoned nickel catalyst. *J. Catal.,* 21(2), pp. 171-178.

Rönkkönen, H. et al., 2010. Catalytic clean-up of gasification gas with precious metal catalysts – A novel catalytic reformer development. *Fuel,* Volume 89, pp. 3272-3277.

Rönkkönen, H. et al., 2011. Precious metal catalysts in the clean-up of biomass gasification gas Part 1: Monometallic catalysts and their impact on gasification gas composition. *Fuel Process. Technol.,* Volume 92, pp. 1457-1465.

Sansaniwal, S., Pal, K., Rosen, M. & Tyagi, S., 2017. Recent advances in the development of biomass gasification technology: A comprehensive review. Volume 72, pp. 363–384.

Sato, K. & Fujimoto, K., 2007. Development of new nickel based catalyst for tar reforming with superior resistance to sulfur poisoning and coking in biomass gasification. *Catal. Commun.,* Volume 8, pp. 1697-1701.

Seim, H. et al., 1997. Deposition of LaNiO3 thin films in an atomic layer epitaxy reactor. *J. Mater. Chem.,* 7(3), pp. 449-454.

Seville, J., 1997. *Gas cleaning in demanding applications.* 1st ed. Glasgow: Chapman & Hall .

Seville, J., Chuah, T. G., Sibanda, V. & Knight, P., 2003. Gas cleaning at high temperatures using rigid ceramic filters. *Adv. Powder Technol.,* 14(6), pp. 657–672.

Sharma, S. D. et al., 2010. Recent developments in dry hot syngas cleaning processes. *Fuel,* Volume 89, pp. 817-826.

Sharma, S. D. et al., 2008. A critical review of syngas cleaning technologies — fundamental limitations and practical problems. *Powder Technol.,* Volume 180, pp. 115-121.

Shen, Y., Wang, J., Ge, X. & Chen, M., 2016. By-products recycling for syngas cleanup in biomass pyrolysis - An overview. *Renew. Sust. Energ. Rev.,* Volume 56, pp. 1246-1268.

Siedlecki, M. et al., 2009. Effect of Magnesite as Bed Material in a 100 kWth Steam-Oxygen Blown Circulating Fluidized-Bed Biomass Gasifier on Gas Composition and Tar Formation. *Energ. Fuels,* Volume 23, pp. 5643-5654.

Sie, S. & Krishna, R., 1999. Fundamentals and selection of advanced Fischer-Tropsch reactors. *Appl. Catal. A-Gen.,* pp. 55-70.

Sikarwar, V. S. et al., 2017. Progress in biofuel production from gasification. *Prog. Energ. Combust.,* Volume 61, pp. 189-248.

Simell, P. et al., 2014. Clean syngas from biomass - process development and concept assessment. *Biomass Conv. Bioref.,* Volume 4, pp. 357-370.

Simell, P., Kurkela , E. & Ilkka , H., 2015. *Method of reforming gasification gas.* United States, Patent No. US 8,936,658 B2.

Simell, P., Kurkela, E., Ståhlberg, P. & Hepola, J., 1996. Catalytic hot gas cleaning of gasification gas. *Catal. Today,* 27(1-2), pp. 55-62.

Simeone, E. et al., 2010. Study of the Behaviour of a Catalytic Ceramic Candle Filter in a Lab-Scale Unit at High Temperatures. *Int. J. Chem. React. Eng.,* Volume 8, pp. 1-19.

Simeone, E. et al., 2011. Filtration performance at high temperatures and analysis of ceramic filter elements during biomass gasification. *Biomass Bioenerg.,* Volume 35, pp. 87-104.

Simeone, E. et al., 2013. High temperature gas filtration with ceramic candles and characterisation during steam-oxygen blown gasification. *Fuel,* Volume 108, pp. 99-111.

Spath, P. & Dayton, D., 2003. *Preliminary Screening — Technical and Economic Assessment of Synthesis Gas to Fuels and Chemicals with Emphasis on the Potential for Biomass-Derived Syngas,* Golden, Colorado: National Renewable Energy Laboratory.

Speight, J. G., 2011. *Biofuels Handbook.* Cambridge: Royal Society of Chemistry.

Srinakruang, J., Sato, K., Vitidsant, T. & Fujimoto, K., 2005. A highly efficient catalyst for tar gasification with steam. *Catal. Commun.,* Volume 6, pp. 437-40.

Stevens, D. J., 2001. *Hot Gas Conditioning: Recent Progress With Larger-Scale Biomass Gasification Systems,* Golden, Colorado: National Renewable Energy Laboratory.

Succi, M., Zilio, S. & Bonucci, A., 2008. *Fumes Treatment System.* US, Patent No. US 20080209898 A1.

Sutherland, K., 2008. *Filters and Filtration Handbook.* 5th ed. Burlington: Elsevier Ltd..

Sutton, D., Kelleher, B. & Ross, J. R., 2001. Review of literature on catalysts for biomass gasification. *Fuel Process. Technol.,* Volume 73, pp. 155-173.

Swierczynski, D., Libs, S., Courson, C. & Kiennemann, A., 2007. Steam reforming of tar from a biomass gasification process over Ni/olivine catalyst using toluene as a model compound. *Appl. Catal. B,* Volume 74, pp. 211-222.

Swisher, J. et al., 1996. Properties of sulfur sorbents containing dispersed nickel in an Al2O3 matrix. *J. Mater. Eng. Perform.,* 5(2), pp. 247-255.

Szemmelveisz, K. et al., 2009. Examination of the combustion conditions of herbaceous biomass. *Fuel Process. Technol.,* Volume 90, pp. 839-847.

Tijmensen, M. J., Faaij, A. P., Hamelinck, C. N. & van Hardeveld, M. R., 2002. Exploration of the possibilities for production of Fischer Tropsch liquids and power via biomass gasi%cation. *Biomass Bioenerg.,* Volume 23, pp. 129 – 152.

Tomishige, K. & Fujimoto, K., 1998. Ultra-stable Ni catalysts for methane reforming by carbon dioxide. *Catal. Surv. Jpn,* Volume 2, pp. 3-15.

Tomishige, K. et al., 2003. Catalyst performance in reforming of tar derived from biomass over noble metal catalysts. *Green Chem.,* Volume 5, pp. 399-403.

Torres, W., Pansare, S. S. & Goodwin Jr., J. G., 2007. Hot Gas Removal of Tars, Ammonia, and Hydrogen Sulfide from Biomass Gasification Gas. *Catal. Rev.,* 49(4), pp. 407-456.

Tortorelli, P. F., McKamey, C. G., Lara-Curzio, E. & Judkins, R. R., 1999. Iron-aluminide filters for hot-gas cleanup. *Am. Soc. Mech. Eng.,* pp. 1-6.

Trimm, D. L., 1985. Poisoning of Metallic Catalysts. In: *Deactivation and Poisoning of Catalysts.* USA: s.n., pp. 151-184.

Tuomi, S., Kurkela, E., Simell, P. & Reinikainen, M., 2015. Behaviour of tars on the filter in high temperature filtration of biomass-based gasification gas. *Fuel,* Volume 139, pp. 220-231.

Wakker, J. P., Gerritsen, A. W. & Moulijn, J. A., 1993. High Temperature H2S and COS Removal with MnO and FeO on yA1203 Acceptors. *Ind. Eng. Chem. Res.,* Volume 32, pp. 139-149.

Wang , T., Chang, J. & Lv, P., 2005 . Novel Catalyst for Cracking of Biomass Tar. *Energy Fuel,* 19(1), pp. 22-27.

Wang, G. et al., 2017. Desulfurization and tar reforming of biogenous syngas over Ni/olivine in a decoupled dual loop gasifier. *Int. J. Hydrogen Energ.,* 42(23), pp. 15471-15478.

Wang, S. & Lu, G. Q., 1996. Carbon Dioxide Reforming of Methane To Produce Synthesis Gas over Metal-Supported Catalysts: State fo the Art. *Energy Fuel,* Volume 10, pp. 896-904.

Vassilatos, V., Taralas , G., Sjöström, K. & Björnbom, E., 1992. Catalytic cracking of tar in biomass pyrolysis gas in the presence of calcined dolomite. *Can. J. Chem. Eng.,* 70(5), pp. 1008-1013.

Weerachanchai, P., Horio, M. & angsathitkulchai, C., 2009. Effects of gasifying conditions and bed materials on fluidized bed steam gasification of wood biomass. *Bioresource Technol.,* Volume 100, pp. 1419-1427.

Westmoreland , P. R. & Harrison, D. P., 1976. Evaluation of Candidate Solids for Hihg-Temperature Desulfurization of Low-Btu Gases. *Environ. Sci. Technol.,* 10(7), pp. 659-661.

Wilhelm, D. J., Simbeck, D. R., Karp, A. D. & Dickenson, R. L., 2001. Syngas production for gas-to-liquids applications: technologies, issues and outlook. *Fuel Process. Technol.,* Volume 71, pp. 139-148.

Villot, A. et al., 2012. Separation of particles from syngas at high-temperatures with an electrostatic precipitator. *Sep. Purif. Technol.,* Volume 92, pp. 181-190.

Woolcock, P. J. & Brown, R. C., 2013. A review of cleaning technologies for biomass-derived syngas. *Biomass Bioenerg.,* Volume 52, pp. 54-84.

Xiao, G. et al., 2013. Granular bed filter: A promising technology for hot gas clean-up. *Powder Technol.,* Volume 244, pp. 93-99.

Yu, Q., Brage, C., Chen, G. & Sjöström, K., 1996. Temperature impact on the formation of tar from biomass pyrolysis in a free-fall reactor. *J. Anal. Appl. Pyrol.,* Volume 40-41, pp. 481-489.

Zennaro, R. et al., 2013. Syngas: The Basis of Fischer-Tropsch. In: P. M. Maitlis & A. de Klerk, eds. *Greener Fischer-Tropsch Processes: for Fuels and Feedstocks.* Weinheim: Wiley-VCH Verlag GmbH & Co., pp. 19-52.

Zevenhoven & Kilpinen, 2004. Filter systems. In: *Particulates*, pp. 5-33.

Zhang, Y., Draelants, D. J., Engelen, K. & Baron, G. V., 2003. Development of nickel-activated catalytic filters for tar removal in H2S-containing biomass gasification gas. *J. Chem. Technol. Biotechnol.,* Volume 78, pp. 265-268.

Zhang, Y., Ma, L., Wang, T. & Li, X., 2016. MnO2 coated FE2O3 spindles designed for production of C5+ hydrocarbons in Fischer-Tropsch synthesis. *Fuel,* Volume 177, pp. 197-205.

Zhao, H., Draelants, D. J. & Baron, G. V., 2000. Performance of a Nickel-Activated Candle Filter for Naphthalene Cracking in Synthetic Biomass Gasification Gas. *Ind. Eng. Chem. Res.,* Volume 39, pp. 3195-3201.

Zhou, C., Rosén, C. & Engvall, K., 2016. Biomass oxygen/steam gasification in a pressurized bubbling fluidized bed: Agglomeration behavior. *Appl. Energ.,* Volume 172, pp. 230-250.

Zhou, C., Rosén, C. & Engvall, K., 2017. Selection of dolomite bed material for pressurized biomass gasification in BFB. *Fuel Process. Technol.,* Volume 159, pp. 460-473.

APPENDIX 1

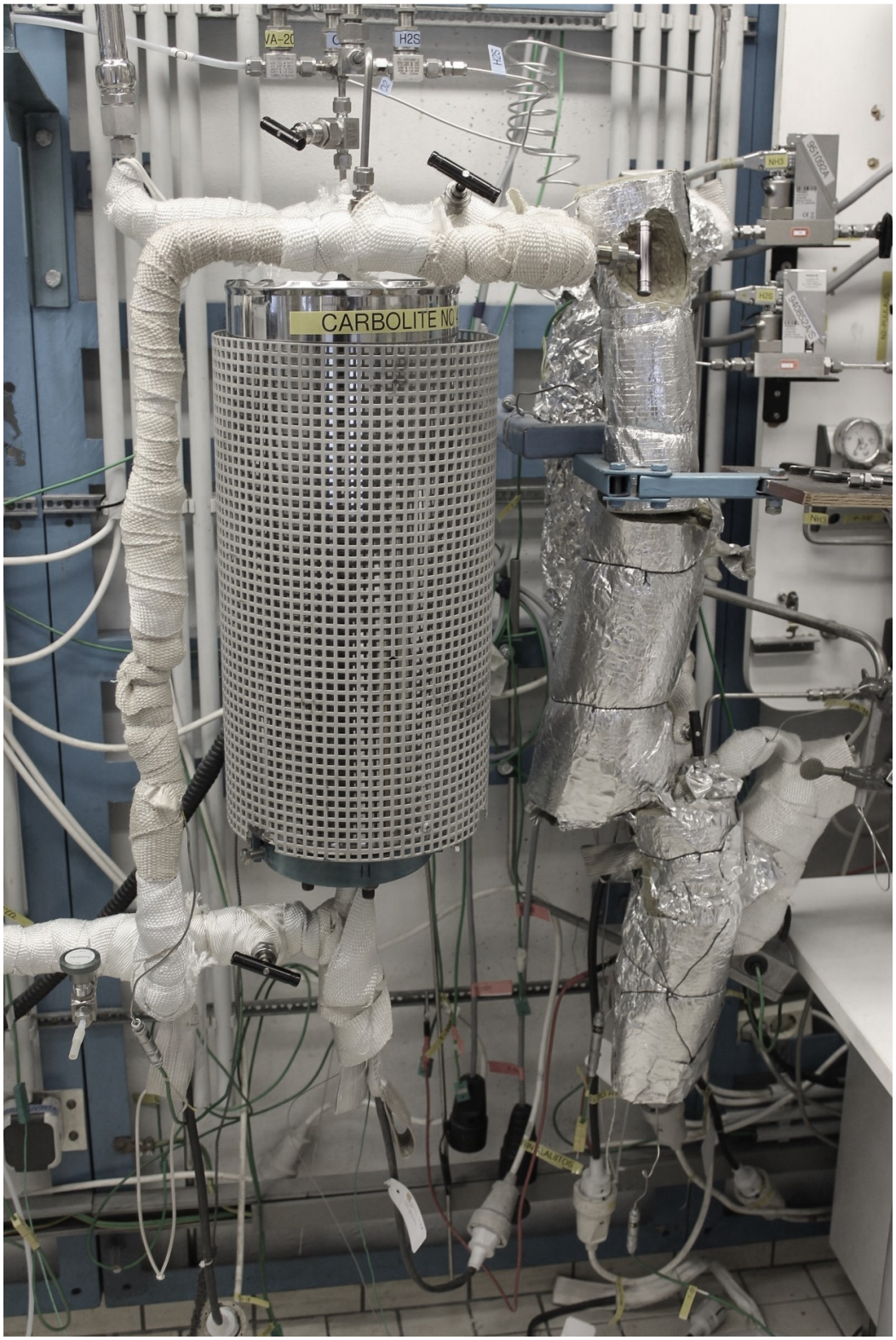

Figure 1. Experimental setup of the pressurized plug flow reactor surrounded by a three-zone furnace.

APPENDIX 2

Table 1. Gas and liquid components used in the experiments.

Component	Producer	Level of purity (%)
CO	AGA	99.97
CO_2	AGA	99.99
CH_4	AGA	99.995
H_2	AGA	99.999
C_2H_4	AGA	99.95
N_2	AGA	99.999
Benzene	Merck	> 99.7
Toluene	Merck	≥ 99.9
Naphthalene	Merck	> 99
H_2S	AGA	0.5000 mol-% in N_2

Table 2. Mass flow meters used in the experiments.

Gas	Maximum gas flow (l/min)	Model	Producer
CO	0.5	F-201C-FB-33-V	Bronkhorst
CO_2	2.5	F-201CV-5K0-ABD-33-Z	Bronkhorst
CH_4	0.5	F-201CV-500-ABD-33-V	Bronkhorst
H_2	5	F-201CV-5K0-ABD-33-V	Bronkhorst
H_2S	0.05	F-201C-FB-33Z	Bronkhorst
C_2H_4	0.5	F-201C-FB-33Z	Bronkhorst
N_2	2	F-201DV-2K0-ABD-33-V	Bronkhorst

Table 1. Conditions and filters for the experiments.

Run	Feeding gas	Reactor temperature (˚C)	Pressure (bar)	Filter configuration	Gas velocity (l/min)
2	Nitrogen	60	1	Empty reactor	1.0, 1.5 and 2.0
4	Gas mixture	700, 800 and 900	1	Empty reactor	1.5
5	Nitrogen	60	1	Filter without a catalyst	1.0, 1.5 and 2.0
6	Gas mixture	700, 800 and 900	1	Filter without a catalyst	1.5
7	Gas mixture	700, 800 and 900	3	Filter without a catalyst	1.5
8	Gas mixture	700, 800 and 900	5	Filter without a catalyst	1.5
9	Nitrogen	60	1	Nickel	1.0, 1.5 and 2.0
10	Gas mixture	700, 800 and 900	1	Nickel	1.5
11	Gas mixture	700, 800 and 900	3	Nickel	1.5
12	Gas mixture	700, 800 and 900	5	Nickel	1.5
13	Gas mixture	700, 800, 850 and 900	5	Nickel and alumina	1.5
14	Gas mixture	700, 800, 850 and 900	5	Nickel and alumina	1.5
15	Gas mixture	700, 800, 850 and 900	5	Filter without a catalyst	1.0
16	Gas mixture	700, 800, 850 and 900	3	Filter without a catalyst	1.5
17	Gas mixture	700, 800, 850, 875 and 900	5	Filter without a catalyst	0.75
18	Gas mixture	700, 800, 850 and 900	5	Nickel	1.5
19	Gas mixture without H_2S	800, 850, 875 and 900	5	Nickel and alumina	1.0
20	Gas mixture	800, 850, 875 and 900	5	Nickel and alumina	1.0
21	Gas mixture	800, 850, 875 and 900	5	Nickel and alumina	1.0
22	Gas mixture	800, 850, 875 and 900	5	Nickel and alumina	1.5
24	Gas mixture	800, 850, 875 and 900	5	Filter without a catalyst	1.5
25	Gas mixture	800, 850, 875 and 900	5	Nickel and alumina	0.75
26	Gas mixture	800, 850, 875 and 900	5	Nickel	1.5
27	Gas mixture	800, 850, 875 and 900	5	Nickel and alumina	1.5

Table 2. Filters used in the experiments and the weights of formed cake on the filter.

Run	Filter number	Porosity (μm)	Catalyst	Weight of the filter cake (mg)
5	M3000417, 1.4767 mod.2	100-200	Filter without a catalyst	-
6	M3000417, 1.4767 mod.2	100-200	Filter without a catalyst	21
7	M3000417, 1.4767 mod.2	100-200	Filter without a catalyst	59
8	M3000416, 1.4767 mod.2	160-300	Filter without a catalyst	84
9	M3000417, 1.4767 mod.2	100-200	16-18 nm NiO	200
10	M3000418, 1.4767 mod.2	200-300	16-18 nm NiO	250
11	M3000418, 1.4767 mod.2	200-300	18-21 nm NiO	210
12	M3000417, 1.4767 mod.2	100-200	19-21 nm NiO	210
13	M3000418, 1.4767 mod.2	200-300	35-39 nm NiO and 11-12 nm Al_2O_3 bottom	214
14	M3000419, 1.4767 mod.2	75-100	17-13 nm NiO, 21-24 nm Al_2O_3 top	118
15	M3000419, 1.4767 mod.2	75-100	Filter without a catalyst	123
16	M3000419, 1.4767 mod.2	75-100	Filter without a catalyst	71
17	M3000418, 1.4767 mod.2	200-300	Filter without a catalyst	154
18	M3000417, 1.4767 mod.2	100-200	35-39 nm NiO	346
19	M3000417, 1.4767 mod.2	100-200	35-39 nm NiO and 11-12 nm Al_2O_3 bottom	350
20	M3000416, 1.4767 mod.2	160-300	60-65 nm NiO and 11-12 nm Al_2O_3 bottom	357
21	M3000416, 1.4767 mod.2	160-300	35-39 nm NiO and 11-12 nm Al_2O_3 bottom	386
22	M3000419, 1.4767 mod.2	75-100	60-65 nm NiO and 11-12 nm Al_2O_3 bottom	299
24	M3000416, 1.4767 mod.2	160-300	Filter without a catalyst	221
25	M3000418, 1.4767 mod.2	200-300	35-39 nm NiO and 11-12 nm Al_2O_3 bottom	57 (oxidized)
26	M3000418, 1.4767 mod.2	200-300	35-39 nm NiO	295
27	M3000418, 1.4767 mod.2	200-300	35-39 nm NiO and 11-12 nm Al_2O_3 bottom	325

Table 1. Conversions and yields for the experiments without a catalyst.

Run	Set point temperature (˚C)	Conversion (%)				Gas Yield (%)				Pressure drop (mbar)
		C_6H_6	C_7H_8	$C_{10}H_8$	C_2H_4	H_2	CO	CO_2	CH_4	
4	700	-1	0	-3	-2	-1	-1	0	1	Not recorded
	800	-6	5	-3	8	-2	-1	0	4	
	900	-50	56	-2	18	-3	0	0	10	
6	700	0	1	-1	1	-2	0	0	4	Not recorded
	800	-6	4	1	-3	-2	-1	-2	4	
	900	-41	48	1	12	-3	-1	-2	10	
7	700	-3	0	3	4	-3	-2	-2	3	Not recorded
	800	-39	46	7	41	-11	-7	-6	4	
	900	-87	99	-4	47	-8	-2	-3	24	
8	700	5	12	8	23	-3	-2	-1	-7	Not recorded
	800	-62	84	9	66	-17	-11	-10	0	
	900	-59	99	8	78	-8	1	0	29	
15	700	21	29	2	25	-5	-3	-3	-2	157
	800	-12	69	3	61	-13	-7	-7	7	190
	850	-18	95	6	73	-6	1	1	26	154
	900	-50	99	20	68	-10	0	-3	33	187
16	700	2	5	6	7	-1	0	0	0	99
	800	-33	41	7	37	-9	-5	-5	-1	129
	850	-73	85	4	38	-9	-4	-4	8	187
	900	-76	98	4	45	-5	0	-1	20	397
17	700	8	26	1	33	3	5	5	6	97
	800	-38	59	1	56	1	6	5	16	153
	850	-51	91	14	66	-9	-1	-3	23	168
	875	-47	97	26	73	-6	2	0	31	150
	900	-46	99	29	75	-5	4	0	35	195
24	800	-27	58	2	54	-14	-9	-7	-5	133
	850	-45	93	5	57	-13	-6	-5	19	194
	875	-60	98	9	64	-10	-2	-2	27	314
	900	-53	99	17	67	-7	2	0	29	466

Table 2. Conversions and yields for the filters with a catalyst.

Run	Set point T (°C)	Conversion (%)				Gas Yield (%)				Pressure drop (bar)
		C_6H_6	C_7H_8	$C_{10}H_8$	C_2H_4	H_2	CO	CO_2	CH_4	
10	700	0	1	0	0	0	0	0	0	
	800	-3	5	0	2	-1	0	0	1	Not recorded
	900	-40	54	8	17	0	2	-1	5	
11	700	-2	2	2	6	-1	-1	0	0	65
	800	-35	39	2	25	0	2	2	7	70
	900	-75	99	10	57	-2	4	0	26	1807
12	700	-12	-5	2	7	-1	0	0	1	121
	800	-56	71	0	57	2	6	6	14	152
	900	-94	99	28	63	-2	6	0	33	1108
13	700	-13	-6	3	7	-1	0	0	1	122
	800	-61	47	1	45	-1	4	4	11	159
	850	-122	85	4	51	-4	2	1	22	1280
	900	-71	99	46	88	3	12	2	39	3036
14	700	-15	-2	3	14	-12	-7	-8	7	127
	800	-55	69	4	62	-11	-7	-7	2	124
	850	-93	83	4	53	-2	4	3	20	131
	900	-72	98	12	70	0	6	4	31	156
19	800	-43	65	23	65	-13	-7	-9	7	210
	850	-47	95	20	72	-6	1	-5	27	233
	875	-71	97	25	69	-6	3	-6	27	228
	900	-56	99	32	74	-5	6	-4	36	250
20	800	-19	69	4	59	2	8	7	15	144
	850	-30	95	14	67	2	8	6	28	267
	875	-26	99	32	75	-3	5	0	32	1123
	900	-7	99	55	85	1	13	0	42	2013
21	800	-27	71	1	62	-14	-8	-7	5	169
	850	-41	95	12	65	-10	-3	-4	23	245
	875	-45	99	29	76	-6	4	-1	35	1082
	900	-19	100	53	94	0	12	1	45	2207
22	800	-46	57	6	50	-8	-5	-4	2	145
	850	-75	98	11	52	-5	0	-1	18	1566
	875	-66	99	33	84	-3	8	0	41	3459
	900	-45	99	54	96	-3	15	-3	48	4044
25	800	-47	85	3	67	-15	-8	-6	15	127
	850	-58	98	7	72	-11	-2	-3	29	137
	875	-53	99	17	76	-8	2	-2	34	177
	900	-44	99	30	84	-6	7	-4	36	181

Experiment 20 Setup 1

IN

Dry gas

Analyzer values	vol-%
CO	17.69
CO2	28.17
CH4	4.77
H2	43.84
O2	0.00
N2	2.52
H2O	0.00
NH3	0.00
H2S	0.01
C2H4	3.00

Gas chromatography	ppm	
Benzene	1956.00	
Toluene	1434.00	
Naphthalene	253.00	Sum
		100.00

Wet gas

Calculated	vol-%
CO	9.78
CO2	15.57
CH4	2.64
H2	24.24
O2	0.00
N2	1.39
H2O	44.34
NH3	0.00
H2S	0.01
C2H4	1.66

Calculated	vol-%	
Benzene	0.20	
Toluene	0.14	
Naphthalene	0.03	Sum
		100.00

OUT

Dry gas

Analyzer values	vol-%
CO	18.13
CO2	28.66
CH4	5.33
H2	42.50
O2	0.00
N2	0.57
H2O	0.00
NH3	3.64
H2S	0.01
C2H4	1.16
C2H6	0.00

Gas chromatography	ppm	
Benzene	2320.28	
Toluene	448.96	
Naphthalene	242.62	Sum
		100.00

Wet gas

Calculated	vol-%
CO	10.59
CO2	16.75
CH4	3.12
H2	24.84
O2	0.00
N2	0.33
H2O	41.25
NH3	2.13
H2S	0.01
C2H4	0.68
C2H6	0.00

Calculated	vol-%	
Benzene	0.23	
Toluene	0.04	
Naphthalene	0.02	Sum
		100.00

Volumetric flows (l/min)

	Dry	Wet
In	0.83	1.50
Out	0.88	1.50
Water	0.6651	0.6182
Tars	0.0055	0.0045

Balances

	C	H	N	O	S
In	1.36	6.30	0.11	3.42	0.00
Out	1.36	6.25	0.11	3.42	0.00
In/Out	1.00	1.01	1.00	1.00	1.00
%	100.00	100.84	99.81	100.00	100.00

Conversions X (%)

C2H4	59.03	CO	7.59
Benzene	-18.52	CO2	6.93
Toluene	68.72	CH4	15.32
Naphthalene	4.18	H2	2.33
H2O	7.05		

Ratios

	In	Out
H2/H2O	0.55	0.60
CO/CO2	0.63	0.63
H2/CO	1.56	1.48

In	(mol/s)	Out	(mol/s)
CO	0.39	CO	0.43
CO2	0.63	CO2	0.67
CH4	0.11	CH4	0.13
H2	0.97	H2	1.00
O2	0.00	O2	0.00
N2	0.06	N2	0.01
H2O	1.78	H2O	1.66
H2S	0.00	H2S	0.00
C6H6	0.01	Benzene	0.01
C7H8	0.01	Toluene	0.00
C10H8	0.00	Naphthalene	0.00
C2H4	0.07	C2H4	0.03
C2H6	0.00	C2H6	0.00
NH3	0.00	NH3	0.09
	4.02		4.01

Feeding gas values from results
Product gas values from results
Changing variable cells

	M [g/mol]	d [kg/dm3n]
H2	2.02	
CH4	16.04	
O2	32.00	
N2	28.00	
C2H4	28.05	
NH3	17.02	
H2S	34.09	
Benzene	78.05	0.88
Toluene	92.13	0.65
Naphthalene	128.16	1.15
Vesi	18.02	1.00

Gas chromatography

IN		OUT	
Compound	Average [vol-ppm]	Compound	Average [vol-ppm]
C6H6, Benzene	1956	C6H6, Benzene	2320
CH4	50000	CH4	53345
C7H8, Toluene	1434	C7H8, Toluene	449
C2H6	0	C2H6	41111
C2H4	30000	C2H4	11638
C2H2	0	C2H2	11
C3H4	0	C3H4	0
1-C4H8	0	1-C4H8	4
t-2-C4H8	0	t-2-C4H8	0
1,3-C4H6	0	1,3-C4H6	0
C-2-C4H8	0	C-2-C4H8	186
N-C5H12	0	N-C5H12	0
1-Buten-3-yne	0	1-Buten-3-yne	0
1-C5H10	67	1-C5H10	202
C10H8, Naphthalene	253	C10H8, Naphthal	243

Gas analyzer

IN		OUT	
CO	17.69	CO	18.13
CO2	28.17	CO2	28.66
CH4	4.77	CH4	5.46
H2	43.84	H2	42.50
O2	0.01	O2	0.01

		Error			Error
C6H6, Benzen	0.20	0.00	C6H6, Benzene	0.23	0.00
C7H8, Toluene	0.15	0.00	C7H8, Toluene	0.04	0.00
C10H8, Naphth	0.03	0.00	C10H8, Naphthaler	0.02	0.00
Total tars	0.37	0.00	Total tars	0.29	0.01
H2O	44.34	0.00	H2O	41.25	0.00
	g/m3n			g/m3n	
C6H6, Benzen	12.33	25.68	C6H6, Benzene	13.67	19.14
C7H8, Toluene	10.67	Error	C7H8, Toluene	3.12	Error
C10H8, Naphth	2.67	0.00	C10H8, Naphthaler	2.35	0.00
Total tars	25.68		Total tars	19.14	
H2O	644.94		H2O	560.92	

Figure 1. Example of mass balance calculation sheet.